Selective enrichment on a wide polysaccharide spectrum allowed isolation of novel metabolic and taxonomic groups of haloarchaea from hypersaline lakes

Sorokin, Dimitry Y.; Elcheninov, Alexander G.; Khijniak, Tatiana V.; Kolganova, Tatiana V.; Kublanov, Ilya V.

DOI
10.3389/fmicb.2022.1059347

Publication date
2022

Document Version
Final published version

Published in
Frontiers in Microbiology

frontiers | Frontiers in Microbiology

TYPE Original Research
PUBLISHED 23 November 2022
DOI 10.3389/fmicb.2022.1059347

OPEN ACCESS

EDITED BY
Rosa María Martínez-Espinosa,
University of Alicante, Spain

REVIEWED BY
Vikram Hiren Raval,
Gujarat University, India
Heng-Lin Cui,
Jiangsu University, China

*CORRESPONDENCE
Dimitry Y. Sorokin
soroc@inmi.ru;
d.sorokin@tudelft.nl

SPECIALTY SECTION
This article was submitted to Extreme Microbiology, a section of the journal Frontiers in Microbiology

RECEIVED 01 October 2022
ACCEPTED 07 November 2022
PUBLISHED 23 November 2022

CITATION
Sorokin DY, Elcheninov AG, Khijniak TV, Kolganova TV and Kublanov IV (2022) Selective enrichment on a wide polysaccharide spectrum allowed isolation of novel metabolic and taxonomic groups of haloarchaea from hypersaline lakes.
Front. Microbiol. 13:1059347.
doi: 10.3389/fmicb.2022.1059347

Selective enrichment on a wide polysaccharide spectrum allowed isolation of novel metabolic and taxonomic groups of haloarchaea from hypersaline lakes

Dimitry Y. Sorokin[1,2]*, Alexander G. Elcheninov[1], Tatiana V. Khijniak[1], Tatiana V. Kolganova[3] and Ilya V. Kublanov[1,4]

[1]Winogradsky Institute of Microbiology, Federal Research Centre of Biotechnology, Russian Academy of Sciences, Moscow, Russia, [2]Department of Biotechnology, Delft University of Technology, Delft, Netherlands, [3]Institute of Bioengineering, Federal Research Centre of Biotechnology, Russian Academy of Sciences, Moscow, Russia, [4]Faculty of Biology, Lomonosov Moscow State University, Moscow, Russia

Extremely halophilic archaea (haloarchaea) of the class *Halobacteria* is a dominant group of aerobic heterotrophic prokaryotic communities in salt-saturated habitats, such as salt lakes and solar salterns. Most of the pure cultures of haloarchaea were enriched, isolated, and cultivated on rich soluble substrates such as amino acids, peptides or simple sugars. So far, the evidences on the capability of haloarchaea to use different polysaccharides as growth substrates remained scarce. However, it is becoming increasingly obvious that these archaea can also actively participate in mineralization of complex biopolymers, in particular cellulose and chitin–two dominant biomass polysaccharides on the planet. Here we used an array of commercially available homo- and heteropolysaccharides to enrich hydrolytic haloarchaea from hypersaline salt lakes with neutral pH and from alkaline soda lakes. This resulted in isolation of a range of halo- and natrono-archaea, respectively, belonging to already described taxa as well as several new genus-level lineages. In some cases, the isolates enriched with different polysaccharides happened to be closely related, thus representing generalistic ecotype, while the others were narrow specialists. In general, soda lakes yielded a broader range of polysaccharide-utilizing specialists in comparison to neutral salt lakes. The results demonstrated a significant diversity of halo(natrono)archaea with a previously unrecognized potential for utilization of a broad range of natural polysaccharides in hypersaline habitats.

KEYWORDS

halo(natrono)archaea, hypersaline lakes, soda lakes, polysaccharides, hydrolytic

Introduction

Hypersaline lakes and solar salterns at its final evaporation stage represent unique salt-saturated habitats dominated by extremely halophilic microbial communities among which the extremely halophilic archaea of the class *Halobacteria* is the particularly successful group (Cui and Dyall-Smith, 2021). These archaea (at least those known in culture) are mostly aerobic organoheterotrophs, utilizing simple soluble organic compounds, such as amino acids and sugars (Andrei et al., 2012; Oren, 2013, 2015; Grant and Jones, 2016). Haloarchaea typically have very high cell density that gives the characteristic reddish color to hypersaline brines in intracontinental athalassic lakes and thalassic endeavaporite pools of the marine solar salt concentrators. Only handful of cultivated haloarchaeal species can grow with polymeric substances, such as starch, proteins or olive oil (Bhatnagar et al., 2005; Enache and Kamekura, 2010; Moshfegh et al., 2013; Selim et al., 2014; Amoozegar et al., 2017). Recently, this spectrum has been expanded by recalcitrant insoluble polysaccharides, such as cellulose and chitin as well as some other partially soluble polysaccharides, such as galactomannan and xylan. Utilization of native insoluble forms of cellulose has recently been shown for the neutrophilic genera *Halococcoides*, *Halomicrobium*, and *Halosimplex* (Sorokin et al., 2015, 2019a, 2020a) and for two genera of natronoarchaea from soda lakes–*Natronolimnobius* and *Natronobiforma* (Sorokin et al., 2015, 2018, 2019b). The ability to use chitin as the growth substrate has been proven for the neutrophilic genera *Halomicrobium* and *Salinarchaeum* and for the natronoarchael genus *Natrarchaeobius* (Sorokin et al., 2015, 2019c, 2020b; Minegishi et al., 2017). Finally, growth with locust bean galacto-beta-1,4-mannan was shown for the neutrophilic genera *Natronoarchaeum* and *Haloarcula* (Shimane et al., 2010; Enomoto et al., 2020).

The potential of haloarchaea to utilize various recalcitrant polysaccharides produced mostly by plants and algae is of significant interest both for fundamental understanding of their functional importance for the organic matter mineralization in hypersaline environments and also by regarding them as a source of extremely halo(alkali)stable extracellular hydrolases which have important application potential in production of biofuel from lignocellulosic wastes because this process often starts with a decrystallization pretreatment step, performed either with alkali or ionic liquids (Kaar and Holtzapple, 2000; Zavrel et al., 2010; Begemann et al., 2011).

In this work, the search for polysaccharide-utilizing haloarchaea was extended beyond the most abundant cellulose and chitin. For this, a range of commercially available polysaccharides of plant and microbial origin was used for selective enrichment and further isolation in pure cultures of halo(natrono)archaea able to utilize these polymers as growth substrate. The *de novo* sequenced genomes of these strains allowed to establish their phylogenies as well as to detect the genes, encoding enzymes responsible for their polysacharidolytic capacities. The results demonstrated significant diversity of polysaccharide-specialized haloarchaea belonging to already described genera and species (mostly for salt lakes) and several new genera (mostly among natronoarchaea), all of which have enzymatic repertoire sufficient for decomposition of the respective polysaccharides.

Experimental procedures

Samples

Sediment (top 3 cm) and brine samples were obtained from five hypersaline chloride-sulfate lakes with neutral pH in Kulunda Steppe (Altai, Russia) and from hypersaline alkaline (soda) lakes in Kulunda Steppe (three lakes), northeastern Mongolia (two lakes) and North America (California, two lakes) (Sorokin et al., 2015). Two "master mixes," one for each type of lakes, were created by mixing equal parts of sediments and brines from each lake and used at 5% (v/v) for primary enrichments.

Enrichment and growth conditions

The neutrophilic haloarchaea originated from salt lakes were enriched, purified and further cultivated in a neutral base medium 1 with the following composition (g l^{-1}): 230 NaCl, 5 KCl, 0.2 NH_4Cl, 2.5 K_2HPO_4, pH 6.8. After sterilization, the base was supplemented with vitamin and trace metal mix (Pfennig and Lippert, 1966) (1 ml l^{-1} each) and 2 mM $MgSO_4$. For the soda lake enrichments and further cultivation of alkaliphilic natronoarchaea, a sodium carbonate/bicarbonate-based medium 2 containing 4 M total Na^+ [(g l^{-1}): 190 Na_2CO_3, 30 $NaHCO_3$, 16 NaCl, 5 KCl and 1 K_2HPO_4, final pH 10 after sterilization] was supplemented with the same additions as for the medium 1, except that the amount of Mg was two times lower and that 4 mM NH_4Cl was added after sterilization. This alkaline medium was mixed 1:3 with the neutral medium 1, resulting in the final pH of 9.6.

Polysaccharides (Sigma-Aldrich and Megazyme; **Supplementary Table 1**) were either added from suspensions in sterile distilled water (when heat sterilization was not possible) or from 5% heat-sterilized (110°C for 20 min) stocks to a final concentration of 0.5 g l^{-1}. At the stage of initial enrichments and further 1:100 transfers, a mixture of streptomycin and kanamycin (final concentration 100 mg l^{-1}) was added to suppress bacterial development. Cultivation was performed in 30 ml bottles sealed with gray-rubber septa (to prevent evaporation) containing 10 ml medium at 35°C on a rotary shaker at 150 rpm. Solid media were prepared by 3:2 (v:v)

mixing of the fully prepared liquid media with 4% washed agar at 50°C. Solid NaCl was added to the portions of liquid media before heating to bring the salinity back to 4 M of total Na^+ after agar addition. For isolation of pure cultures, the initial positive enrichments were passed 2 times into new media containing target polysaccharides at 1:100 dilution to obtain sediment-free cultures, followed with dilution to extinction series and finally plating the maximal positive dilutions onto solid media with the same composition. The dominant colony types or those showed visible signs of polymer degradation (where possible) were picked up with sterile Pasteur capillary with pooled tips under control of binocular and placed into liquid media. Only those cultures which showed vigorous growth in liquid media were further purified by repeating the colony formation procedure. The purity of isolates were confirmed by microscopy, 16S-rRNA gene sequencing (Sanger and amplicon profiling) and in several cases by full genome sequencing.

Polysaccharide utilization activity

The main indication of polysaccharide utilization was consistent microbial growth in liquid culture whereby the polysaccharide in question served as the sole carbon and energy source. In addition, whenever it was possible, the hydrolytic activities of spot-colonies were also visualized on agar plates, either by formation of clearance zones (amorphous cellulose, beta-mannan) or reagent-developed hydrolysis zone: Lugol solution for starch, pullulan and pectin and Congo Red/1 M NaCl for xylan, xyloglucan, arabonoxylan, and glucomannan.

Genomic sequencing and phylogenetic analysis

Genomic DNA isolation, DNA library preparation, sequencing as well as genome assembly were performed as described earlier (Sorokin et al., 2022a).

Phylogenomic analysis based on the "ar122" set of conserved single copy archaeal proteins (Rinke et al., 2021) was performed as follows: the protein sequences were identified and aligned in *in silico* proteomes of the type species of all genera within *Halobacteria* class (non-type species were taken for *Halalkalicoccus* and *Natronoarchaeum* genera because the genomes of the type species were not available) using the GTDB-tk v.1.7.0 with reference data v.202 (Chaumeil et al., 2019). The maximum likelihood tree was inferred using the RAxML v.8.2.12 (Stamatakis, 2014) with the PROTGAMMAILG model of amino acid substitution; support values were calculated from the 1000 rapid bootstrap replications. The phylogenetic tree was polished using iTOL v.6.5.8 (Letunic and Bork, 2019).

Genome analysis

The genomes were annotated with NCBI Prokaryotic Genome Annotation Pipeline (Tatusova et al., 2016). Carbohydrate-active enzymes (CAZymes) including glycosidases, polysaccharide lyases, carbohydrate esterases, glycosyl transferases, and carbohydrate oxidases genes were predicted using dbCAN2 script v2.0.11 (Zhang et al., 2018) with HMMER v3.3 (Mistry et al., 2013) with default thresholds. The most probable activities of identified CAZymes (excluding glycosyl transferases, for which the manual verification of the predictions was not performed) were predicted using BLAST search against Swiss-Prot database (Boutet et al., 2016).

Genbank accession numbers

The 16S rRNA gene sequences generated in this study were deposited in the GenBank under accession numbers ON787970-ON788000. The whole genome sequence are available in GenBank under the following accession numbers: JAOPJY000000000, JAOPJZ000000000, JAOPKA000000000, JAOPKB000000000, JAOPKC000000000, JAOPKD000000000, and JAOPKE000000000.

Results

Polysaccharide-utilizing haloarchaea from hypersaline lakes with neutral pH

Positive enrichment cultures from salt lakes were obtained with 13 out of 18 polysaccharide compounds tested. The fastest development (maximal growth yield was achieved after 1 week) was observed with starch-like compounds (amylopectin, pullulan, and glycogen), while the slowest (up to a month)–with insoluble beta-linked polysaccharides (beta-mannan and curdlan). Other positive cultures showed growth in between 2 and 3 weeks. All positive primary enrichments were transferred into a sediment-free stage after 2–3 consecutive 1:100 (v:v) transfers on the same synthetic medium and acquired pink coloration with a domination of polymorphic flat cells characteristic of haloarchaea accompanied by visible degradation of substrates in case of insoluble polysaccharides. Further dilutions to extinction were performed without antibiotics and were generally positive up to 10^{-8}–10^{-9}. Final purification was achieved by isolation of individual colonies on solid media. Pure cultures of polysacharidolytic haloarchaea were obtained from those colony morphotype(s) (not always dominant ones) which consistently grew back in liquid medium with the target polysaccharide used in the enrichment. The list of isolates is given in **Table 1**.

All isolates selected on alpha-bonded polysaccharides belonged to the well-characterized genera of haloarchaea, for some of which utilization of starch is known. However, to our knowledge, the capacity to utilize arabinan and arabinoxylan has never been shown/tested for any cultivated species of haloarchaea. This is also true for *Halorhabdus tiamateia*, a broadly-specialized polysaccharidolytic haloarchaeon, according to our current results (**Table 1**) and previous studies (Wainø and Ingvorsen, 2003; Werner et al., 2014). However, its ability to grow on levan (beta-fructan) was not known before. Isolates belonging to the genus *Natronoarchaeum* were second after *Halorhabdus* by the number of isolated strains and were selected with four polysaccharides, including pullulan, beta-galactan, galactomannan, and curdlan. While utilization of galactomannan has already been reported for *N. mannanilyticum* (Shimane et al., 2010), growth with beta-1,4-galactan and beta-1,3-glucans, such as curdlan, have never been observed in any pure cultures of haloarchaea. Same is true for other two beta-1,4-bonded polysaccharides, including xyloglucan and beta-mannan. Looking from the taxonomical perspective, only two insoluble polysaccharides, mannan (consisted of beta-1,4-linked mannose) and curdlan (consisted of beta-1,3-linked glucose) (**Table 1**) resulted in selection of new genus-level isolates from the neutral salt lakes.

The cross-specificity for various polysaccharides supporting growth of the neutrophilic haloarchaea selected with a single polymer is shown in **Figure 1**. All five species enriched on alpha-glucans utilized soluble starch and five out of the six alpha-glucan specialists also grew with arabinoxylan which has alpha-bonded arabinose residues in the side chains. In

TABLE 1 Polysaccharide-utilizing neutrophilic haloarchaea enriched and isolated from hypersaline salt lakes with neutral pH.

Polysaccharide	Isolates	Identification by 16S rRNA gene sequence		Spectrum of utilized polysaccharides	
		Closest cultured relative	% identity	Stable growth in liquid culture	Colony activity (zone of hydrolysis, mm/2–3 weeks)
Alpha-glucans					
Amylopectin	HArc-St	*Natrinema salaciae*	99	Amp/Sst/Glc/Arx	nd/41/nd
Pullulan	HArc-pul1	*Haloferax alexandrinus*	100	Pul/Sst/Arx	30/20/nd
	HArc-pul2	*Natronoarchaeum rubrum*	99	Pul/Sst/Arx/Gtm/Glt/Crd	45/50/nd
Glycogen	HArc-glc1	*Halorubrum alkalophilum*	99	Glc/Sst	nd/22
	HArc-glc2	*"Halobacterium hubeiense"*	99	Glc/Sst/Arx	nd/15
Arabinan	HArc-arb1-5	*"Halobacterium hubeiense"*	99	Arb/Arx/Xyl	nd/40/20
Dextran	No isolates; not utilized by any isolates				
Beta-fructans					
Levan	HArc-lev	*Halorhabdus tiamatea*	99	Lev/Sst/Arx/Pul/Xyl	nd/23
Inulin	No isolates; not utilized by any isolates				
Beta-bonded polysaccharides					
Pectic galactan	HArc-glct1	*Natronoarchaeum rubrum*	99	Glt/Pul/Sst/Arx/Pul/Xyl	20/30/10/20/20/30
Beta-mannan	**HArc-m1***	*Halovarius/Haloterrigena*	**94–95**	Man/Gcm/Arx/Xyl/Xgl/Ac	20/20/30/30/nd/32/15
Glucomannan	HArc-gm1/3/4	*Halorhabdus tiamatea*	99	Pul/Sst/Arx/Xyl	30/40/30/30
	HArc-gm2	*Halomicrobium zhouii*	99	Gcm/Man/Arx/Xyl/Ac/Lam/Bgl	20/8/40/30/7/nd/nd
Galactomannan	HArc-glctm2	*Haloarcula hispanica*	97.3	Gtm/Glt/Pul/Sst	nd/nd/18/12
	HArc-glctm4	*Natronoarchaeum rubrum*	99		
Xylan	HArc-x1/2	*Halorubrum tebenquichense*	100	Xyl/Arx	30/22
Xyloglucan	HArc-xlg1	*Halorhabdus tiamatea*	99.8	Xgl/Arx/Xyl	nd/25/10
Arabinoxylan	HArc-ax1/3	*Halorhabdus tiamatea*	99.7	Pul/Sst/Arx/Xyl	27/34/25/32
Curdlan	HArc-curdl1	*Haloferax sulfurifontis*	97.6	Crd/Pch/Lam/Pul(w)	nd
	HArc-curdl4	*Natronoarchaeum rubrum*	99	Crd/Pch/Lam/Pul(w)	nd/nd/nd/16
	HArc-curdl5-1	*Halapricum salinarum*	**95**	Crd/Pch/Lam/Sst(w)/Inl/Glc	nd
Arabinogalactan	No isolates; not utilized by any isolates				
Alginate					
Pectin					

Polysaccharides: Sst, soluble starch; Glc, glycogen; Pul, pullulan; Lev, levan; Inl, inulin; Amp, amylopectin; Arb, arabinan; Arx, arabinoxylan; Gcm, glucomannan; Gtm, galactomannan; Glt, galactan; Xyl, xylan; Xlg, xyloglucan; Ac, amorphous cellulose; Lam, laminarin; Crd, curdlan; Pch, pachyman; Blg, Barley glucan; nd, test is not possible; potential new genera are in bold. *This isolate was similar to AArc-m2/3/4 isolated on mannan from soda lakes (see **Table 2**).

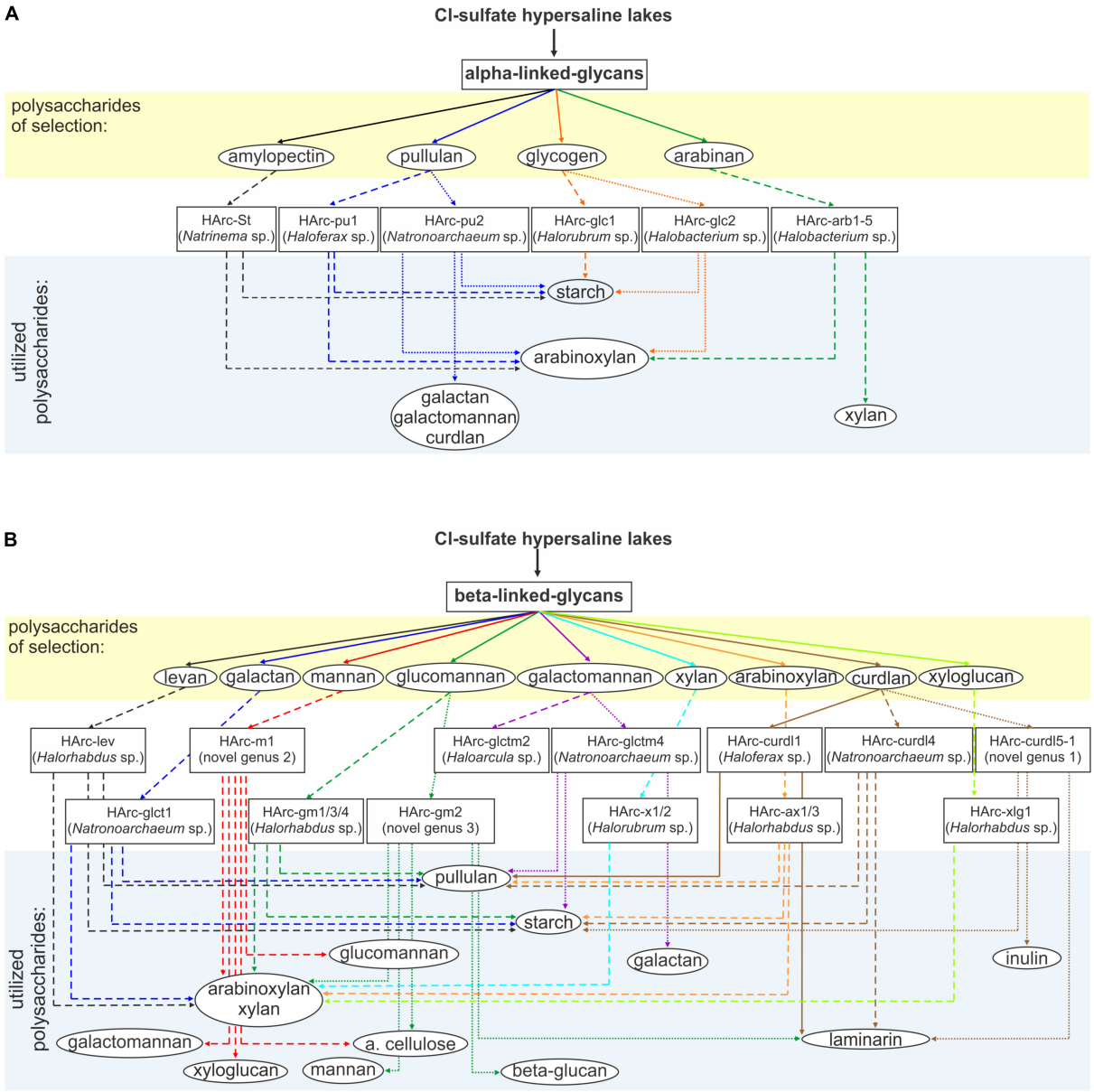

FIGURE 1
Schematic representation of selective enrichments of haloarchaea from hypersaline salt lakes on **(A)** alpha-bonded and **(B)** beta-bonded polysaccharides. Assignment to the novel genus was based on protein sequence-based phylogenomic analysis and 16S rRNA gene sequence identity values.

turn, a single case of cross-specificity was also observed in *Halobacterium* strains which were selected with both glycogen (HArc-glc2) and arabinan (HArc-arb1-5) (Figure 1A).

Among the haloarchaeal strains selected with various beta-bonded polysaccharides the most common cross-substrates were xylan and arabinoxylan, while alpha-glucans (starch and pullulan) were only utilized by a few beta-glucan specialists (Figure 1B). Two out of the three isolates enriched with either mannan (HArc-m1) or glucomannan (HArc-gm2) were able to grow with amorphous cellulose indicating related selectivity of these beta-1,4 backbone polysaccharides. The *Halomicrobium* strain HArc-gm2 selected with glucomannan was identical in its 16S rRNA gene sequence to *Halomicrobium* sp. HArcel3–the cellulose-enriched haloarchaeon most closely related to *H. zhouii* (Sorokin et al., 2015). We tested the type strain *H. zhouii* JCM 17095 and it appeared to be able to grow with amorphous cellulose as well.

Strain HArc-m1 was identical (according to the 16S rRNA gene sequence analysis) to several natronoarchaeal isolates enriched from soda lakes with beta-1,4 mannan

backbone polysaccharides (see below) confirming a link between the cellulose and the beta-mannan selectivity. This pattern has already been observed in cellulotrophic *Natronobiforma cellulositropha* which was enriched on cellulose but can also grow with beta-mannan (Sorokin et al., 2018). Furthermore, HArc-m1 is the only strain enriched from the neutral salt lakes being closely related to isolates from soda lakes representing quite a rare example in our long-term work with hypersaline lakes. It is also worth to notice that, in this particular case, the substrate selectivity (mannan) overruled the dominant selective factor – the nature of sodium salt (chloride vs. carbonate) and, therefore, the considerable difference in the pH-osmotic pressure combination. Growth experiments confirmed that strain HArc-m1 can indeed grow both at neutral pH and up to pH 9.5, thus being a facultative alkaliphile.

Polysaccharide-utilizing natronoarchaea from hypersaline soda lakes

Positive stable enrichment cultures from soda lakes were obtained with 14 out of 16 polysaccharides tested (pullulan and arabinogalactan were not tested). Similar for salt lakes, alginate and pectin enrichments were negative. Another similarity was the fastest growth (1 week) of the starch-like alpha-glucans (amylopectin and glycogen) and the slowest growth (up to a month) of the insoluble beta-linked-glycans (beta-mannan and curdlan) and α-1,6-glucan dextran (which was negative in case of salt lake samples) utilizing enrichment cultures. However, in contrast to salt lakes further dilution to extinction from the soda lake enrichments had still to be done in the presence of antibiotics since in their absence the cultures were rapidly overrun by bacteria. It was even necessary to add antibiotics to the solid media at the final stage of pure culture isolation. The contaminating bacteria mostly belonged to the genus *Halomonas* which were unable to grow on the target polysaccharide but most probably scavenged the hydrolysis products. The *Halomonas* colonies were easily distinguished from the pink-orange colonies of natronoarchaea which helped to purify the latter, although, in most cases only 1-2 types of such colonies grew back in the liquid medium with the target polysaccharide. The list of isolated polysaccharide-utilizing natronoarchaea is given in **Table 2**.

Four different alpha-bonded glucans and fructans resulted in selection of seven isolates, of which, all except two belonged to know genera. Two isolates enriched and isolated either on amylopectin or inulin were identical in their 16S rRNA gene sequences and represented a novel genus and species *Natronocalculus amylovorans* (Sorokin et al., 2022a). The other three amylopectin-utilizing isolates were closely related to each other and to a facultively anaerobic sulfur-respiring amylolytic *Natranaeroarchaeum sulfidigenes* (Sorokin et al., 2022b). Together with the isolate AArc-lev selected with beta-fructan–levan (**Table 2**) those four strains have recently been described as a new species *Natranaeroarchaeum aerophilus* (Sorokin et al., 2022b). So, there seems to be a connection in starch-like alpha-glucans and beta-fructans selectivity among natronoarchaea.

Interestingly, although glycogen is structurally similar to amylopectin (both are branched alpha-glucans), the two glycogen-selected natronoarchaeal isolates from the genera *Natronococcus* and *Natronorubrum* were not related to above-mentioned new taxa. But all four were able to grow with soluble starch and pullulan, similar to the members of the genus *Natronococcus* which are well-known for their ability to utilize starch and to produce alkalistable amylases (Kobayashi et al., 1992; Kanal et al., 1995).

To our knowledge, dextrans have never been shown or even suspected to support growth of any known *Halobacteria* species, while it was mentioned among positive substrates in anaerobic hyperthermophilic archaea *Desulfurcococcus fermentas* (Perevalova et al., 2005), *D. kamchatkensis* (Kublanov et al., 2009), *Thermoccoccus sibiricus* (Mardanov et al., 2009), and *Thermococcus* sp. strain 2319 × 1 (Gavrilov et al., 2016). While starch-like polysaccharides can have side branches with alpha-bonded glucose other than α-1,4, none but dextrans have the α-1,6 backbone, which probably makes them difficult substrates for hydrolytic archaea. From two forms of the cyanobacterial dextran tested in this work (19.5 and 200 kDa), only the low molecular weight variety resulted in a positive enrichment and isolation of a single natronoarchaeal strain AArc-dxtr1 representing a distant novel species in the genus *Saliphagus* (**Table 2**).

Finally, an alpha-1,5-arabinan enrichment from soda lakes yielded a stable binary culture impossible to separate by serial dilutions. Plating showed two distinctive types of colonies: a dominant type with small red colonies and less abundant larger and nearly colorless colonies. Both grew back in liquid pure cultures with arabinan. Interestingly, the arabinan utilization in the liquid culture inoculated with the colorless colonies resulted in a formation of soluble yellow-brownish product, while the red colonies culture supernatant remained colorless. The isolate AArc-arb3/5 with colorless colonies was identified as a novel *Natrialba* species (with the highest 16S rRNA sequence identity of 97% to "*N. wudunaoensis*"), while the second isolate AArc-arb1/2/6 with red colonies was closely related to the known species *Natronolimnobius baerhuensis*.

The natronoarchaea selected from soda lakes on various beta-bonded polysaccharides can be divided into two major groups: preferably xylanolytic and cellulo-/mannanolytic (**Table 2**). The xylanolytics selected on either xylan, arabinoxylan and galactan belonged to the known genus *Natronolimnobius*. Xyloglucan, galactomannan, and mannan

10.3389/fmicb.2022.1059347

TABLE 2 Polysaccharide-utilizing natronoarchaea enriched and isolated from hypersaline soda lakes.

Polysaccharide	Isolates	Identification by 16S rRNA gene sequence		Spectrum of utilized polysaccharides	
		Closest cultured relative	% identity	Stable growth in liquid culture	Colony activity (zone of hydrolysis, mm/2–3 weeks)
Alpha-glucans					
Amylopectin	AArc-St1-1	*"Natranaeroarchaeum*	99.4	Amp/Sst/Pul/Cdx/Lev	nd/35/23/nd/nd
	AArc-St1-2	*sulfidigenes"*	98.5	Amp/Sst/Pul/Cdx/Inl	nd/19/15/nd/nd
	AArc-St1-3	*"Natronocalculus*	99.1		
	AArc-St2	*amylolyticus"*	**100**		
Pullulan	Was not tested since AArc-St isolates were able to utilize pullulan				
Glycogen	AArc-glc1/2/4	*Natronococcus amylolyticus*	99	Glc/Sst/Arx/Xyl/Gcm	nd/23/25/15/20
	AArc-glc3	*Natronorubrum tibetense*	100	Glc/Sst	nd/25
Dextran	**AArc-dxtr1**	*Saliphagus infecundisoli*	96.8	Dxt/Arx/Sst(w)/Inl/Gcm(w)	nd/30/12/nd/8
Arabinan	AArc-arb1/2/6	*Natronolimnobius baerhuensis*	99	Arb/Arx/Arg/Xyl/Gcm(w)	nd/30/nd/9/11/5
	AArc-arb3/5	*Natrialba magadii*	96.4	Arb/Arx/Xyl	nd/15/25
Beta-fructans					
Levan	AArc-lev1	= AArc-St1-1	99	Lev/Sst	nd/20
Inulin	AArc-in1	= AArc-dxtr1	99.8	Inl/Sst/Dxt (weak)	nd/20/nd
	AArc-in2	=AArc-St2		Inl/Sst//Pul	nd/15/20
Beta-bonded polysaccharides					
Pectic galactan	AArc-glct1	*Natronolimnobius baerhuensis*	100	Glt/Arx/Xyl/Gcm/Arg	Nd/30/25/10/nd
Beta-mannan	AArc-m1	*Natronococcus amylolyticus*	99	Man/Arx/Xgl/Gcm	18/20/20/25
	AArc-m2/3/4*	*Halovarius/Haloterrigena*	**94–95**	Man/Gcm/Arx/Xyl/Xgl/Ac	20/20/30/30/20/20
	AArc-m6	*Natronobiforma cellulositropha*	100	Man/Arx/Xyl/Gcm/Ac	12/12/10/12/32
Glucomannan	**AArc-gm3/4/5-2**	**=AArc-m2/3/4**	100	Gcm/Man/Arx/Xyl/Cel	15/10/22/18/22
	AArc-gm6	*Natronobiforma cellulositropha*	100		
Galactomannan	**AArc-glctm3/4/8**	*Natronococcus amylolyticum*	99	Gtm/Gcm/Sst/Inl	nd/18/20/nd
	AArc-glctm5	**=AArc-m2/3/4**	**100**		
Xyloglucan	**AArc-xg1-1**	**=AArc-m2/3/4**	**100**	Xgl/Xyl/Arx/Ac/Man	15/7/22/12/8
Xylan arabinoxylan	AArc-x1/2/3/4	*Natronolimnobius baerhuensis*	99	Xyl/Arx/Ac/Sst	35/18/12/18
	AArc-ax1/2/3		99	Arx/Xyl/Arg	30/20/nd
Curdlan	**AArc-curdl1**	*Halostagnicola alkaliphila*	**95**	Crd/Pch/Lam/Gtm/Sst	nd/nd/nd/nd/15
Arabinogalactan	Was not tested since several other AArc isolates were able to utilize it				
Alginate	No isolates; not utilized by any isolates				
Pectin	There was some growth in primary enrichment but it was not reproduced further in sediment-free transfers				

See Table 1. w, weak growth; *This isolate was similar to HArc-m1 isolated on mannan from salt lakes (see Table 1). Bold values indicate potentially new genera.

enrichments were all dominated by a novel genus-level lineage to which a facultatively alkaliphilic strain HArc-m1 (see above; Table 2) also belonged. Furthermore, a less abundant component in the galactomannan enrichment was identified as a member of the genus *Natronococcus*. A dominant organism in a glucomannan enrichment was identical to the cellulose/mannan-specialized *Natronobiforma cellulositropha* (Sorokin et al., 2018). This is similar to the selectivity of glucomannan in salt lakes resulted in isolation of a cellulolytic haloarchaeon HArc-gm2 closely related to cellulotrophic *Halomicrobium* HArcel3 dominating in cellulose enrichments from hypersaline lakes (Sorokin et al., 2015).

Curdlan, a beta-1,3-glucan homopolysacharide, selected a single natronoarchael strain representing a new genus lineage of the polysaccharide-utilizing archaea. The enrichment culture was very slow in development resulting in degradation of antibiotics and massive development of bacteria belonging to *Halomonas*. Several repeated attempts with sequential addition of antibiotics resulted in the sufficient enrichment of the archaeal component appropriate for further purification on a solid medium. Despite its general chemical similarity to cellulose, curdlan molecules have a different physical structure (helical in contrast to flat ribbon cellulose fibrils) (Deslandes et al., 1980). Altogether, its structural characteristics, both primary and secondary, as well as low occurrence in nature makes it highly selective substrate in comparison with the more common beta-1,4 glucans. We did not manage to find any published data on curdlan utilization in haloarchaea. On the other hand, two out of ten CAZymes families (GH81 and GH16) including members with the endo-β-1,3-glucanase activities (EC 3.2.1.39) have archaeal representatives. While archaeal representatives of the GH81 family are known exclusively by the presence of the respective genes in their genomes, a single archaeal GH16 glycosidase from *Pyrococcus furiosus* (Gueguen et al., 1997) was characterized as a laminarinase able to hydrolyze laminarin, lichenan, and barley β-glucan. However, no information of its capability to hydrolyze curdlan was provided. It should be noted that the halo- and natronoarchaea enriched and isolated on curdlan in the course of this work were capable to grow on laminarin, a soluble beta-1,3/1,6 glucan.

The growth cross-specificity for various polysaccharides among the natronoarchaeal isolates is shown in **Figure 2**. From the strains isolated on alpha-bonded polysaccharides, the amylolytics were most restricted in their polymer-utilizing profiles with only beta-fructans as the alternative substrates. The only exception was *Natronococcus* AArc-glc1/2/4, isolated on glycogen and able to grow with a few beta-1,4 bonded polysaccharides. On the other hand, strains selected with other alpha-bonded polysaccharides, such as dextran and arabinan, were all able to utilize xylan and arabinoxylan and one of them also grew with arabinogalactan (**Figure 2A**).

Among the strains selected with beta-bonded polysaccharides, the most narrowly specialized was strain AArc-curdl1 isolated on curdlan: it only grew with two other polysaccharides with the beta-1,3-backbone (pachyman and laminarin) and on starch (**Figure 2B**). In contrast, the natronoarchaea enriched with various beta-1,4-bonded polysaccharides had a broader substrate range with xylan and arabonoxylan being the most common cross-substrates among them. Similar to the salt lake isolates, the soda lake strains selected with beta-1,4 mannan and glucomannan were also capable of growth on native celluloses. On the other hand, in contrast to salt lakes, the same taxa were also selected on galactomannan. This difference is significant, taking into account importance of cellulose for natural habitats but the reason for this is not clear yet.

Phylogenomic and functional genomic analysis

Genomes of seven stains were *de novo* sequenced and assembled. Quality check of the assemblies revealed high completeness (99–100%) and low contamination (0-1.87%) levels what makes them suitable for both phylogenomic and functional analyses (**Supplementary Table 2**). Genome sizes varied from 2.81 to 5.59 Mbp while the G + C contents for different genomes were 59.2–66%.

Phylogenomic analysis showed that the novel polysaccharidolytic strains are uniformly dispersed within the *Halobacteria* tree (**Figure 3**). Strain AArc-St1-1 belonged to the genus *Natranaeroarchaeum* and is recently described as a new species *N. aerophilus* (Sorokin et al., 2022b), while strain AArc-St2 is described as a novel genus and species *Natronocalculus amylovorans* (Sorokin et al., 2022a). Strain HArc-gm2 was most closely related to the members of the genus *Halosiccatus*. The neutrophilic curdlan-utilizing haloarchaea strains HArc-curdl5-1 and HArc-curdl7 are most closely related to the genus *Halapricum*. The nearest relatives of AArc-dxtr1 are among the *Halostagnicola* species, while AArc-xg1-1, AArc-m2/3/4 and AArc-cudrl1 are related to the cellulolytic *Natronobiforma*. Establishing the exact taxonomic rank (novel species or genus) of these novel haloa(natrono)archaea will need a more in-depth phenotypic and chemotaxonomical characterization.

Polysaccharide-utilizing haloarchaea must have a set of carbohydrate active enzymes (CAZymes), as a prerequisite for successful decomposition of insoluble and soluble poly- and oligosaccharides. Indeed, the sequenced genomes encoded all types of the CAZymes: glycosidases (GH), polysaccharide lyases (PL), glycosyl transferases (GT), carbohydrate esterases (CE), carbohydrate oxidases (AA) as well as carbohydrate-binding modules (CBM). The detailed analysis was focused on GHs and PLs (**Figure 4**; **Supplementary Table 3**) due to their major role in polysaccharide depolymerization.

Closely related neutrophilic strains HArc-curld5-1 and HArc-curdl7 enriched on curdlan had identical CAZyme repertoires. Their capability to degrade curdlan as well as pachyman and laminarin is due to the action of endo-beta-1,3(4)-glucanase (GH81), beta-1,3-glucan phosphorylase (GH161) and beta-glucosidase (GH3). Both strains also grew on starch by means of fourteen alpha-amylases (GH13), three oligo-1,6-glucosidases (GH13), two glucoamylases (GH15), and a 4-alphaglucanotransferase encoded in their genomes. The genome of alkaliphilic strain AArc-curld1 also isolated on curdlan had a smaller set of genes for respective enzymes yet it included an essential endo-beta-1,3(4)-glucanase (GH81)

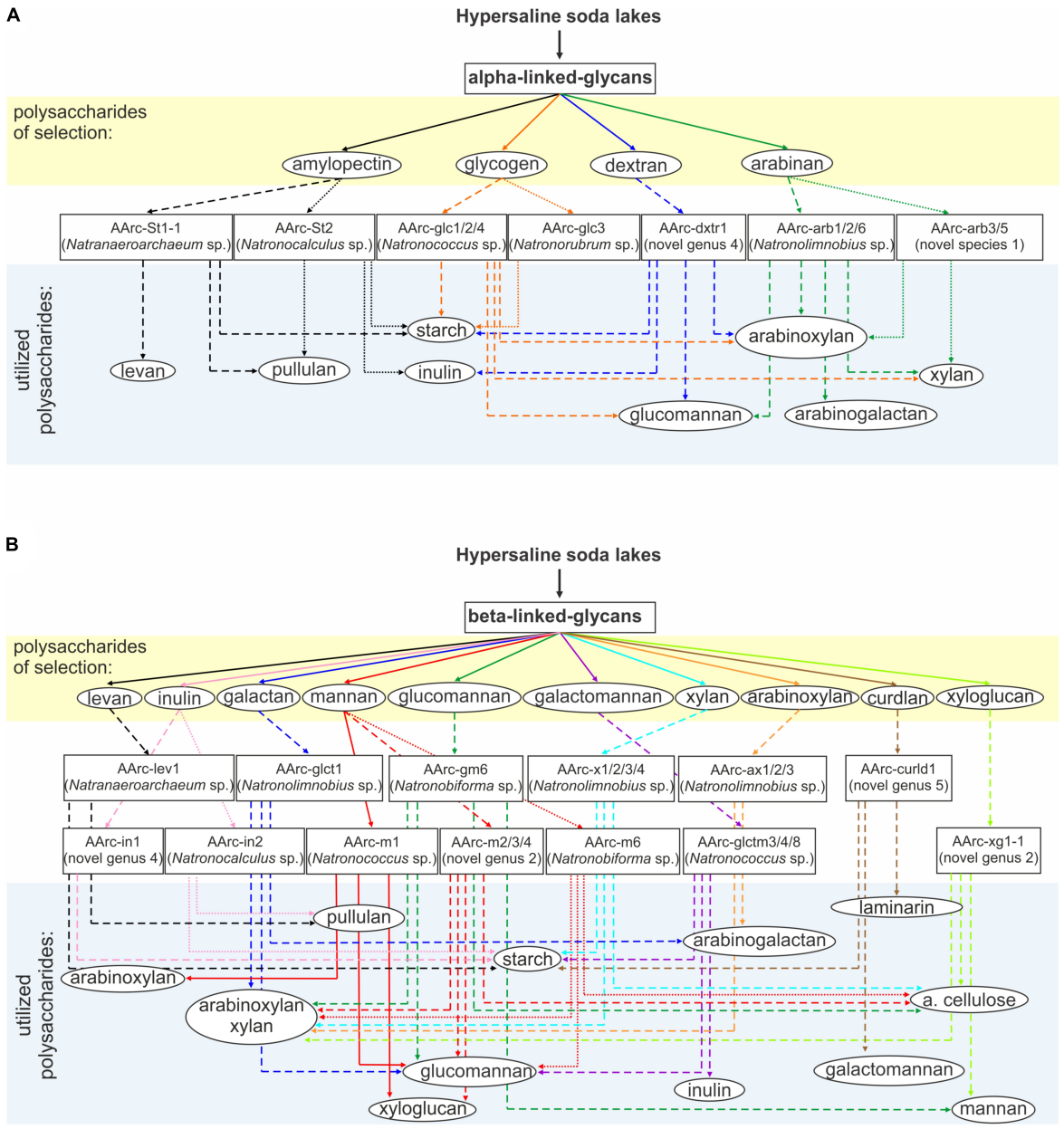

FIGURE 2
Schematic representation of selective enrichments of natronoarchaea from hypersaline soda lakes on **(A)** alpha-bonded and **(B)** beta-bonded polysaccharides. Assignment to the novel genus was based on protein sequence-based phylogenomic analysis and 16S rRNA gene sequence identity values (for strain AArc-arb3/5 only 16S rRNA gene sequence identity values were used).

and a beta-glucosidase (GH3). A neopullulanase (GH13), three alpha-amylases (GH13), a 4-alphaglucanotransferase (GH77), and two glucoamylases (GH15) apparently allowed the strain to utilize soluble starch.

The neutrophilic strain HArcl-gm2 isolated on glucomannan has a machinery for its decomposition including endo-beta-1,4-mannosidase (GH5), several endoglucanases (four from the GH5 and one from the GH9 families), two beta-mannosidases (GH2) and a beta-glucosidase (GH3). The strain also can utilize laminarin and beta-glucan due to the presence of the endo-beta-1,3(4)-glucanase (GH81); xylan and arabinoxylan by means of endoxylanases (seven enzymes from GH10 and three from GH11), beta-xylosidases (GH3), and arabinosidases (GH43 and GH51) responsible for hydrolysis of side chains of arabinoxylan.

Comparative genomic analysis of closely related natronarchaeal strains AArc-xg1-1 (isolated on xyloglucan) and AArc-m2/3/4 (isolated on beta-1,4-mannan) showed

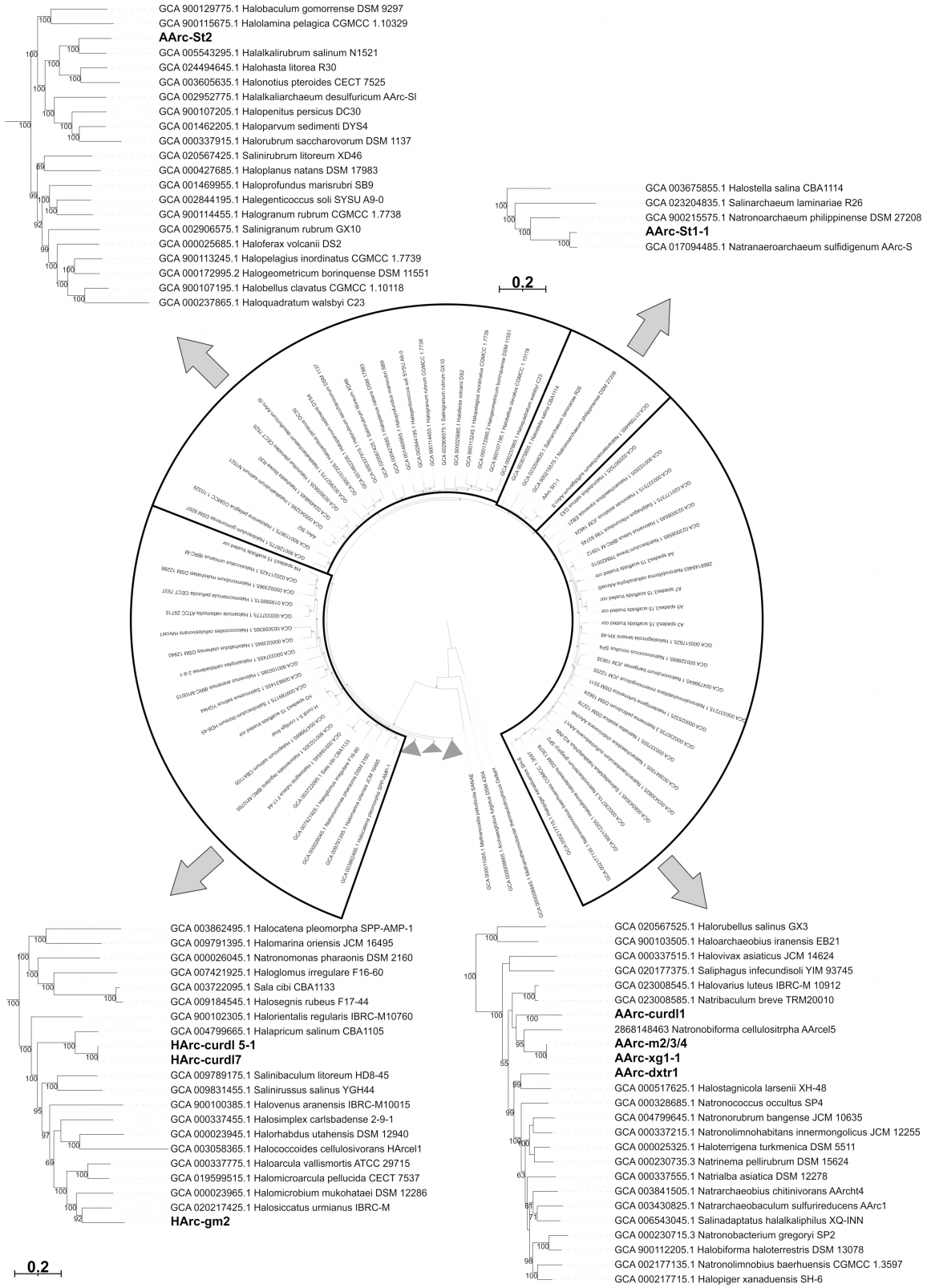

FIGURE 3
Maximum likelihood phylogenomic tree showing position of polysaccharide-utilizing halo(natrono)archaea enriched from hypersaline lakes within the class *Halobacteria*. Sequences of 122 conserved archaeal proteins were used to infer the tree.

10.3389/fmicb.2022.1059347

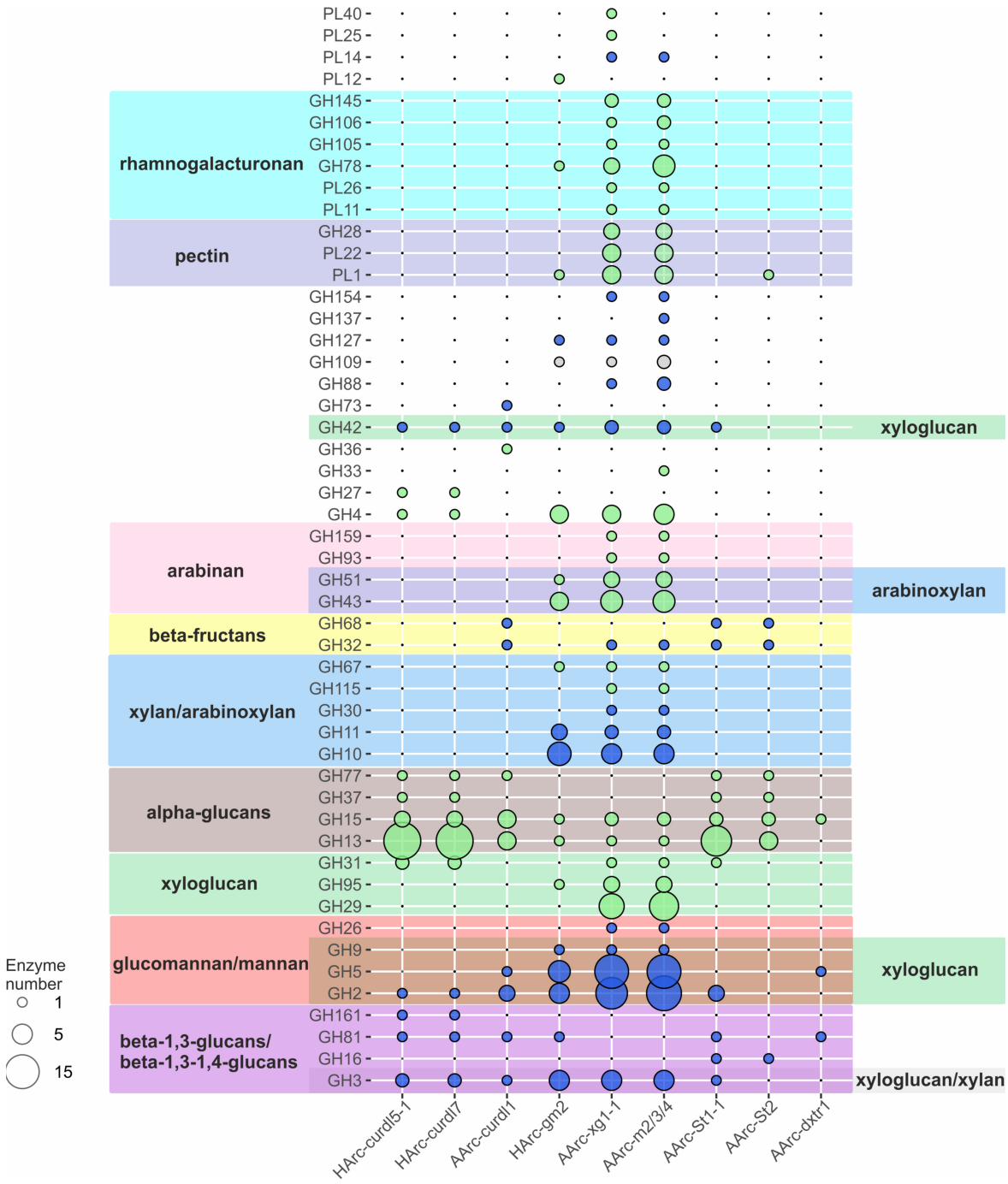

FIGURE 4
Sets of GH and PL genes found in the genomes of novel polysaccharidolytic haloarchaea. Size of bubbles indicate number of enzymes; the color of bubbles indicate the prevailing type of glycosidic bonds hydrolyzed by the enzymes (alpha-bonds—green, beta-bonds—blue, both—gray). Color of background indicates these CAZymes families contains the characterized enzyme(s) capable of depolymerization of respective polysaccharides. No color means the activities, characteristic to these families are not directly linked to the substrates used in this work.

a nearly identical and the largest CAZyme sets among the studied haloarchaea. In particular, the genes encoding several endo-beta-1,4-mannosidases (five enzymes from GH5 family and one from GH26), two beta-mannosidases (GH2), endoglucanases (10 proteins from GH5 and one enzyme from GH9), three beta-glucosidases (GH3 family), endo-beta-1,4-xylanases (5 enzymes from GH10 and two enzymes from GH11), beta-xylosidase (GH3) were found. Moreover, the

genes of enzymes known to degrade galacturonate-containing polymers (polygalacturonate, pectin, rhamnogalacturonan) were also detected: three polygalacturonases (GH28), putative pectate lyases (four proteins from PL1 family and four from PL22), two rhamnogalacturonan lyases (PL11, PL26) as well as arabinan-hydrolyzing enzymes (six proteins from GH43, three GH51 enzymes and one enzyme from GH93). However, none of these isolates grew with either pectins, polygalacturonate, rhamnogalacturonan, or arabinan. This example clearly demonstrates that functional conclusions based solely on the genomic evidence should be considered only as preliminary.

The genome of the natronarchaeal amylolytic strain AArc-St1-1 (*Natranaeroarcheum aerophilus*, Sorokin et al., 2022a) contains a large number of genes coding for alpha-bond degrading glycosidases, including ten alpha-amylases (GH13 family), two oligo-1,6-glucosidases (GH13), 4-alpha-glucanotransferase (GH77), glucoamylase (GH15), and trehalase (GH37). Finally, two beta-fructosidases (GH32 and GH68) were also found, apparently allowing the strain to grow on levan. Also, two beta-1,3(4)-glucanases (GH16, GH81), beta-glucosidase/beta-xylosidase (GH3), beta-mannosidase (GH2), alpha-xylosidase (GH31), and several beta-galactosidases (GH2 and GH42 families) genes were present. Another amylolytic strain AArc-St2 (*Natronocalculus amylovorans*) possessed similar CAZymes set (alpha-glucan-specific enzymes from GH13, GH15 and GH77 families as well beta-fructosidases) but the number of alpha-amylases and oligo-1,6-glucosidases was significantly lower (Sorokin et al., 2020a). Despite the presence of genes for putative GH16 beta-glucanase and PL1 pectate lyase, no growth was observed on their specific substrates including beta-glucan, lichenan, curdlan, pachyman, or pectin.

Only three GH genes and no PL genes were found in the genome of dextran-utilizing natronoarchaeon AArc-dxtr1: trehalase (GH15), endoglucanase (GH5), and beta-1,3(4)-glucanase (GH81). The typical dextran-degrading enzymes from GH13, GH49, GH66, or GH70 families a were not encoded and it might be only speculated that dextran is hydrolyzed as a result of side activity of a GH15 enzyme since this family is known to contain glucodextranases (Mizuno et al., 2004). An endoglucanase and a beta-1,3(4)-glucanase could be responsible for hydrolysis of glucomannan and arabinoxylan which this organism can also utilize.

Altogether, the repertoire of CAZymes within the *in silico* proteomes of the nine polysacharidolytic halo/natronoarchaea analyzed in this work (summarized on **Figure 4**) was mostly consistent with their polysaccharide untilization spectrum. In total, the number of CAZyme genes found in the studied HArcel/AArcel strains greatly varied from 30 (strain AArc-St2) to 160 (strain AArc-m2/3/4). Closely related strains isolated with the same (HArc-curld5-1 and HArc-curdl7) or different (AArc-xg1-1 and AArc-m2/3/4) substrates may have identical or similar CAZymes gene sets indicating that a selection substrate will not necessarily lead to isolation of a distinctive phylogenetic lineage. At the same time, despite that the phylogenetically distant strains enriched and isolated with the same polysaccharide have different CAZymes sets, they all had similar patterns of particular CAZymes responsible for the hydrolysis of selective substrate. Surprisingly, the genomes of several isolates including AArc-xg1-1, AArc-m2/3/4, AArc-St2, and HArc-gm2 also contained polysaccharide lyases genes which are nearly unknown within the Archaeal kingdom. However, the growth experiments revealed that none of those strains can grow on alginate, pectin, polygalacturonate or rhamnogalacturonan indicating that these enzymes might have an unknown activity in halophilic archaea. This is also substantiated by the fact that all our attempts to enrich pectin- or alginate-utilizing haloarchaea failed so far. Among the possible reasons might be that these uronic acids-based polysaccharides are hardly present in hypersaline habitats or that hypersalinity changes the chemical properties and enzyme accessibility of the polymers. On the other hand, the high diversity of hydrolytic haloarchaea with the potential to utilize various polysacchirides with different types of glycosidic bonds indicate that such substrates might be available in hypersaline habitats. One of the most probable source of these polymers are external terrestrial plants growing in the area surrounding hypersaline lakes.

Conclusion

The obtained results allow to significantly extend the knowledge on polysaccharide-utilizing capabilities of haloarchaea and archaea in general. Selective enrichment approach leaded to recover the so called "best-fit" organisms specialized on a narrow-specialized conversion of a particular substrate. In case of polysaccharides, however, most of the haloarchaeal isolates enriched with a certain substrate were still able to utilize several other polymers. It was also found that polymers with the alpha-1,4 or beta-1,4 linkage backbones more often resulted in positive enrichments than with other types of linkage, such as the alpha-1,6- or beta-1,3 bonding. Finally, no haloarchaea, growing on uronic acid-based polysaccharides (pectin and alginate), commonly utilized by bacteria, were isolated.

In the course of this work, the first haloarchaea able to grow on such recalcitrant polysaccharides as dextran, curdlan, xyloglucan, and beta-mannan were isolated. The enlarged variety of polysaccharidolytic halo(natrono)archaea recovered from hypersaline lakes with novel substrate utilization specificities is offering a good opportunity for further studies of their extremely halo(alkali)stable hydrolases, both in fundamental enzymology research and prospective application.

Data availability statement

The datasets presented in this study can be found in online repositories. The names of the repository/repositories and accession number(s) can be found in the article/ **Supplementary material**.

Author contributions

DS and TVKh were responsible for microbiology work. AE and IK analyzed the genomes and run phylogenetic analysis. TVKo was responsible for 16S rRNA gene sequencing and identification of the isolates. DS, AE, and IK wrote the manuscript. All authors contributed to the article and approved the submitted version.

Funding

This work was supported by the Russian Science Foundation (grant 20-14-00250) and by the Russian Ministry of Science and Higher Education (field and primary enrichment work).

Conflict of interest

The authors declare that the research was conducted in the absence of any commercial or financial relationships that could be construed as a potential conflict of interest.

Publisher's note

All claims expressed in this article are solely those of the authors and do not necessarily represent those of their affiliated organizations, or those of the publisher, the editors and the reviewers. Any product that may be evaluated in this article, or claim that may be made by its manufacturer, is not guaranteed or endorsed by the publisher.

Supplementary material

The Supplementary Material for this article can be found online at: https://www.frontiersin.org/articles/10.3389/fmicb.2022.1059347/full#supplementary-material

References

Amoozegar, M. A., Siroosi, M., Atashgahi, S., Smidt, H., and Ventosa, A. (2017). Systematics of haloarchaea and biotechnological potential of their hydrolytic enzymes. *Microbiology* 163, 623–645. doi: 10.1099/mic.0.000463

Andrei, A. Ş, Banciu, H. L., and Oren, A. (2012). Living with salt: Metabolic and phylogenetic diversity of archaea inhabiting saline ecosystems. *FEMS Microbiol. Lett.* 330, 1–9. doi: 10.1111/j.1574-6968.2012.02526.x

Begemann, M. B., Mormile, M. R., Paul, V. G., and Vidt, D. J. (2011). "Potential enhancement of biofuel production through enzymatic biomass degradation activity and biodiesel production by halophilic microorganisms," in *Halophiles and hypersaline environments: Current research and future trends*, eds A. Ventosa, A. Oren, and Y. Ma (Heidelberg: Springer), 341–357.

Bhatnagar, T., Boutaiba, S., Hacene, H., Cayol, J.-L., Fardeau, M.-L., Ollivier, B., et al. (2005). Lipolytic activity from halobacteria: Screening and hydrolase production. *FEMS Microbiol. Lett.* 248, 133–140.

Boutet, E., Lieberherr, D., Tognolli, M., Schneider, M., Bansal, P., Bridge, A. J., et al. (2016). UniProtKB/Swiss-Prot, the manually annotated section of the uniprot knowledgebase: How to use the entry view. *Methods Mol. Biol.* 1374, 23–54. doi: 10.1007/978-1-4939-3167-5_2

Chaumeil, P.-A., Mussig, A. J., Hugenholtz, P., and Parks, D. H. (2019). GTDB-Tk: A toolkit to classify genomes with the genome taxonomy database. *Bioinformatics* 36, 1925–1927. doi: 10.1093/bioinformatics/btz848

Cui, H. L., and Dyall-Smith, M. L. (2021). Cultivation of halophilic archaea (class *Halobacteria*) from thalassohaline and athalassohaline environments. *Mar. Life Sci. Technol.* 3, 243–251.

Deslandes, Y., Marchessault, R. H., and Sarko, A. (1980). Triple-helical structure of (1/3)-b-D-glucan. *Macromolecules* 13, 1466–1471.

Enache, M., and Kamekura, M. (2010). Hydrolytic enzymes of halophilic microorganisms and their economic values. *Rom. J. Biochem.* 47, 47–59. doi: 10.1002/bit.27639

Enomoto, S., Shimane, Y., Ihara, K., Kamekura, M., Itoh, T., Ohkuma, M., et al. (2020). *Haloarcula mannanilytica* sp. nov., a galactomannan-degrading haloarchaeon isolated from commercial salt. *Int. J. Syst. Evol. Microbiol.* 70, 6331–6337. doi: 10.1099/ijsem.0.004535

Gavrilov, S. N., Stracke, C., Jensen, K., Menzel, P., Kallnik, V., Slesarev, A., et al. (2016). Isolation and characterization of the first xylanolytic hyperthermophilic euryarchaeon *Thermococcus* sp. Strain 2319x1 and its unusual multidomain glycosidase. *Front. Microbiol.* 7:552. doi: 10.3389/fmicb.2016.00552

Grant, W. D., and Jones, B. E. (2016). "Bacteria, *Archaea and viruses of soda lakes*," in *Soda Lakes of East Africa*, ed. M. Schagerl (Berlin: Springer International Publishing), 97–147.

Gueguen, Y., Voorhorst, W. G. B., van der Oost, J., and de Vos, W. M. (1997). Molecular and biochemical characterization of an endo-β-1,3-glucanase of the hyperthermophilic archaeon *Pyrococcus furiosus*. *J. Biol. Chem.* 272, 31258–31264.

Kaar, W. E., and Holtzapple, M. T. (2000). Using lime pretreatment to facilitate the enzymic hydrolysis of corn stover. *Biomass Bioenergy* 18, 189–199.

Kanal, H., Kobayashi, T., Aono, R., and Kudo, T. (1995). *Natronococcus amylolyticus* sp. nov., a haloalkaliphilic archaeon. *Int. J. Syst. Bacteriol.* 45, 762–766. doi: 10.1099/00207713-45-4-762

Kobayashi, T., Kanai, H., Hayashi, T., Akiba, T., Akaboshi, R., and Horikoshi, K. (1992). Haloalkaliphilic maltotriose-forming α-amylase from the archaebacterium *Natronococcus* sp. strain Ah-36. *J. Bacteriol.* 174, 3439–3444. doi: 10.1128/jb.174.11.3439-3444.1992

Kublanov, I. V., Bidjieva, S. K. H., Mardanov, A. V., and Bonch-Osmolovskaya, E. A. (2009). *Desulfurococcus kamchatkensis* sp. nov., a novel hyperthermophilic protein-degrading archaeon isolated from a Kamchatka hot spring. *Int. J. Syst. Evol. Microbiol.* 59, 1743–1747.

Letunic, I., and Bork, P. (2019). Interactive tree of life (iTOL) v4: Recent updates and new developments. *Nucleic Acids Res.* 47:W256–W259. doi: 10.1093/nar/gkz239

Mardanov, A. V., Ravin, N. V., Svetlitchnyi, V. A., Beletsky, A. V., Miroshnichenko, M. L., Bonch-Osmolovskaya, E. A., et al. (2009). Metabolic versatility and indigenous origin of the archaeon *Thermococcus sibiricus*, isolated

from a Siberian oil reservoir, as revealed by genome analysis. *Appl. Environ. Microbiol.* 75, 4580–4588. doi: 10.1128/AEM.00718-09

Minegishi, H., Enomoto, S., Echigo, A., Shimane, Y., Kondo, Y., Inoma, A., et al. (2017). *Salinarchaeum chitinilyticum* sp. nov., a chitin-degrading haloarchaeon isolated from commercial salt. *Int. J. Syst. Evol. Microbiol.* 67, 2274–2278. doi: 10.1099/ijsem.0.001941

Mistry, J., Finn, R. D., Eddy, S. R., Bateman, A., and Punta, M. (2013). Challenges in homology search: HMMER3 and convergent evolution of coiled-coil regions. *Nucleic Acids Res.* 41:e121. doi: 10.1093/nar/gkt263

Mizuno, M., Tonozuka, T., Suzuki, S., Uotsu-Tomita, R., Kamitori, S., Nishikawa, A., et al. (2004). Structural insights into substrate specificity and function of glucodextranase. *J. Biol. Chem.* 279, 10575–10583. doi: 10.1074/jbc.M310771200

Moshfegh, M., Shahverdi, A. R., Zarrini, G., and Faramarzi, M. A. (2013). Biochemical characterization of an extracellular polyextremophilic α-amylase from the halophilic archaeon *Halorubrum xinjiangense*. *Extremophiles* 17, 677–687. doi: 10.1007/s00792-013-0551-7

Oren, A. (2013). "Life at high salt concentrations," in *The Prokaryotes: Prokaryotic Communities and Ecophysiology*, eds E. Rosenberg, E. F. DeLong, S. Lory, E. Stackebrandt, and F. Thompson (Berlin: Springer Berlin Heidelberg), 421–440.

Oren, A. (2015). Halophilic microbial communities and their environments. *Curr. Opin. Biotechnol.* 33, 119–124.

Perevalova, A. A., Svetlichny, V. A., Kublanov, I. V., Chernyh, N. A., Kostrikina, N. A., Tourova, T. P., et al. (2005). *Desulfurococcus fermentans* sp. nov., a novel hyperthermophilic archaeon from a Kamchatka hot spring, and emended description of the genus *Desulfurococcus*. *Int. J. Syst. Evol. Microbiol.* 55, 995–999. doi: 10.1099/ijs.0.63378-0

Pfennig, N., and Lippert, K. D. (1966). Über das vitamin B_{12}-bedürfnis phototropher schwefelbakterien. *Arch. Microbiol.* 55, 245–256.

Rinke, C., Chuvochina, M., Mussig, A. J., Chaumeil, P.-A., Davín, A. A., Waite, D. W., et al. (2021). A standardized archaeal taxonomy for the genome taxonomy database. *Nat. Microbiol.* 6, 946–959. doi: 10.1038/s41564-021-00918-8

Selim, S., Hagagy, N., Aziz, M. A., El-Meleigy, E.-S., and Pessione, E. (2014). Thermostable alkaline halophilic-protease production by *Natronolimnobius* innermongolicus WN18. *Nat. Prod. Res.* 28, 1476–1479.

Shimane, Y., Hatada, Y., Minegishi, H., Mizuki, T., and Echigo, A. (2010). *Natronoarchaeum mannanilyticum* gen. nov., sp. nov., an aerobic, extremely halophilic archaeon isolated from commercial salt. *Int. J. Syst. Evol. Microbiol.* 60, 2529–2534. doi: 10.1099/ijs.0.016600-0

Sorokin, D. Y., Elcheninov, A. G., Khizhniak, T. V., Koenen, M., Bale, N. J., Damsté, J. S. S., et al. (2022a). *Natronocalculus amylovorans* gen. nov., sp. nov., and *Natranaeroarchaeum aerophilus* sp. nov., dominant culturable amylolytic natronoarchaea from hypersaline soda lakes in southwestern Siberia. *Syst. Appl. Microbiol.* 45:126336. doi: 10.1016/j.syapm.2022.126336

Sorokin, D. Y., Yakimov, M. M., Messina, E., Merkel, A. Y., Koenen, M., Bale, N. J., et al. (2022b). *Natranaeroarchaeum sulfidigenes* gen. nov., sp. nov., carbohydrate-utilizing sulfur-respiring *Haloarchaeon* from Hypersaline lakes, a member of a new family *Natronoarchaeaceae* fam. nov. in the order *Halobacteriales*. *Syst. Appl. Microbiol.* 45:126356. doi: 10.1016/j.syapm.2022.126356

Sorokin, D. Y., Khijniak, T. V., Kostrikina, N. A., Elcheninov, A. G., Toshchakov, S. V., Bale, N. J., et al. (2018). *Natronobiforma cellulositropha* gen. nov., sp. nov., a novel haloalkaliphilic member of the family *Natrialbaceae* (class *Halobacteria*) from hypersaline alkaline lakes. *Syst. Appl. Microbiol.* 41, 355–362. doi: 10.1016/j.syapm.2018.04.002

Sorokin, D. Y., Khijniak, T. V., Kostrikina, N. A., Elcheninov, A. G., Toshchakov, S. V., Bale, N. J., et al. (2019a). *Halococcoides cellulosivorans* gen. nov., sp. nov., an extremely halophilic cellulose-utilizing haloarchaeon from Hypersaline lakes. *Int. J. Syst. Evol. Microbiol.* 69, 1327–1335. doi: 10.1099/ijsem.0.003312

Sorokin, D. Y., Kublanov, I. V., Elcheninov, A. G., and Oren, A. (2019b). *Natronobiforma. In: Bergey's Manual of Systematics of Archaea and Bacteria*. Hoboken: John Wiley & Sons, Inc, doi: 10.1002/9781118960608.gbm01838

Sorokin, D. Y., Elcheninov, A. G., Toshchakov, S. V., Bale, N. J., Sinninghe Damsté, J. S., Khijniak, T. V., et al. (2019c). *Natrarchaeobius chitinivorans* gen. nov., sp. nov., and *Natrarchaeobius halalkaliphilus* sp. nov., alkaliphilic, chitin-utilizing haloarchaea from hypersaline alkaline lakes. *Syst. Appl. Microbiol.* 42, 309–318. doi: 10.1016/j.syapm.2019.01.001

Sorokin, D. Y., Merkel, A. Y., Kublanov, I. V., and Oren, A. (2020a). *Halococcoides. In: Bergey's Manual of Systematics of Archaea and Bacteria*. Hoboken: John Wiley & Sons, Inc, doi: 10.1002/9781118960608.gbm01944

Sorokin, D. Y., Merkel, A. Y., Kublanov, I. V., and Oren, A. (2020b). *Natrarchaeobius. In: Bergey's Manual of Systematics of Archaea and Bacteria*. Hoboken: John Wiley & Sons, Inc, doi: 10.1002/9781118960608.gbm01945

Sorokin, D. Y., Toshchakov, S. V., Kolganova, T. V., and Kublanov, I. V. (2015). Halo(natrono)archaea isolated from hypersaline lakes utilize cellulose and chitin as growth substrates. *Front. Microbiol.* 6:942. doi: 10.3389/fmicb.2015.00942

Stamatakis, A. (2014). RAxML version 8: A tool for phylogenetic analysis and post-analysis of large phylogenies. *Bioinformatics* 30, 1312–1313. doi: 10.1093/bioinformatics/btu033

Tatusova, T., DiCuccio, M., Badretdin, A., Chetvernin, V., Nawrocki, E. P., Zaslavsky, L., et al. (2016). NCBI prokaryotic genome annotation pipeline. *Nucleic Acids Res.* 44, 6614–6624. doi: 10.1093/nar/gkw569

Wainø, M., and Ingvorsen, K. (2003). Production of β-xylanase and β-xylosidase by the extremely halophilic archaeon *Halorhabdus utahensis*. *Extremophiles* 7, 87–93.

Werner, J., Ferrer, M., Michel, G., Mann, A. J., Huang, S., and Juarez, S. (2014). *Halorhabdus tiamatea*: Proteogenomics and glycosidase activity measurements identify the first cultivated euryarchaeon from a deep-sea anoxic brine lake as potential polysaccharide degrader. *Environ. Microbiol.* 16, 2525–2537. doi: 10.1111/1462-2920.12393

Zavrel, M., Bross, D., Funke, M., Büchs, J., and Spiess, A. C. (2010). High-throughput screening for ionic liquids dissolving (ligno-)cellulose. *Bioresour. Technol.* 100, 2580–2587.

Zhang, H., Yohe, T., Huang, L., Entwistle, S., Wu, P., Yang, Z., et al. (2018). dbCAN2: A meta server for automated carbohydrate-active enzyme annotation. *Nucleic Acids Res.* 46:W95–W101. doi: 10.1093/nar/gky418

Selective enrichment on a wide polysaccharide spectrum allowed isolation of novel metabolic and taxonomic groups of haloarchaea from hypersaline lakes.

Dimitry Y. Sorokin, Alexander G. Elcheninov, Tatjana Khizhniak, Tatjana V. Kolganova and Ilya V. Kublanov

Supplementary data file

Table S1. Polysaccharides used for selective enrichment of aerobic hydrolytic halo(natrono)archaea from hypersaline lakes.

Table S2. Statistics and quality of genome assemblies of isolated polysaccharidolytic haloarchaea.

Table S3. CAZymes genes found in the genomes of polysaccharidolytic halo(natrono)archaea.

Table S1. Polysaccharides used for selective enrichment of aerobic hydrolytic halo(natrono)archaea from hypersaline lakes

Polysaccharide	Source	Structure	Solubility in water
alpha-glucans			
amylopectin	Potato	α-1,4/1,6 glucan (branched)	insoluble
pullulan	*Aureobasidium pullulans*	α-1,4 glucan	soluble
glycogen	Oyster (clam)	α-1,4/1,6 glucan (branched)	partially soluble
dextran	*Leuconostoc*	α-1,6/1,3 glucan	soluble
arabinan	Sugar beat	α-1,5/1,3 polyarabinose	soluble
beta-fructans			
inulin	Tubers of *Chikory*	β-2,1 fructan	soluble
levan	Tymothy grass	β -2,6/2,1 fructan	soluble
beta-glucans			
pectic galactan	Potato	β-1,4 polygalactose	soluble
beta-mannan	Ivory nut	β-1,4 polymannose	insoluble (crystalline)
glucomannan	Konjak	β-1,4 mannan/glucan	insoluble (gel-forming)
galacto-mannan	Locust beans, (*Carob*)	**β-1,4 mannan - main chain** α-1,6 galactan - side chain	insoluble (gel-forming)
xylan	Birch and Beech woods	**β-1,4 polyxylose - main chain**	insoluble
xyloglucan	*Tamarind*	**β-1,4 glucan - main chain** α-1,6 xylane/ β-1,2 galactan/ α-1,2 arabinan - side chains	soluble
arabinoxylan	Rye	**β-1,4 xylan - main chain** α-1,3/1,2/1,5 arabinan - side chains	soluble
curdlan pachyman	*Alcaligenes faecalis* Fungal (*Poria*)	β-1,3 glucans	insoluble
arabinogalactan	Larch wood (*Larix liallii*)	**β-1,3 galactan - main chain** β-1,4/1,6 galactan/ α-1,6 arabinan - side chains	soluble
pectin	Citrus, apples	**β-1,4 galacturonate main chain**	insoluble
Na-alginate	Brown algae	β-1,4 guluronate/mannuronate	soluble

Supplemetary table S2. Statistics and quality of genome assemblies of isolated polysaccharidolytic haloarchaea

Strain	Genome size, Mbp	G+C, %	Number of contigs	N50, bp	Completeness, %	Contamination, %
AArc-dxtr1	2.81	63.3	5	1746851	100	0
AArc-curdl1	4.54	59.2	67	161529	100	1.4
AArc-xg1-1	5.59	62.1	67	201832	100	0.93
AArc-m2/3/4	5.51	62	46	203090	99.07	0.93
H-curdl5-1	3.36	63.1	62	116111	100	0.93
HArc-curdl7	3.38	63	52	159171	100	1.87
HArc-gm2	4.25	66	18	470222	100	0.93

Table S3: strain **AArc-St1-1**

Locus tag	HMMER	Signal peptide (SignalP v6.0)	Function
AArcSt11_00580	GT4(184-324)	-	GT
AArcSt11_01370	GH13(315-673)	Tat/SPI	alpha-amylase
AArcSt11_01380	GH13_32(67-338)	Tat/SPI	alpha-amylase
AArcSt11_03715	GH13_32(137-389)	Tat/SPII	alpha-amylase
AArcSt11_03720	GH13_20(293-645)	-	alpha-amylase
AArcSt11_04055	GT4(183-322)	-	GT
AArcSt11_04060	GT2_Glycos_transf_2(4-169)	-	GT
AArcSt11_05065	GH13_32(72-338)+CBM13(491-625)	Tat/SPI	alpha-amylase
AArcSt11_05620	GT2_Glycos_transf_2(6-134)	-	GT
AArcSt11_05715	GH13(270-561)	Tat/SPI	alpha-amylase
AArcSt11_07220	GH37(20-499)	-	trehalase
AArcSt11_07290	GH16(51-284)	Tat/SPII	beta-glucanase
AArcSt11_07650	GH15(287-667)	-	unknown
AArcSt11_07655	GH13(288-567)	-	alpha-amylase
AArcSt11_08270	GH13_20(306-629)	-	alpha-amylase
AArcSt11_08330	GH13(43-322)	no or Sec/SPI	alpha-amylase
AArcSt11_08825	GH15(287-650)+GH15(993-1388)	-	glucoamylase
AArcSt11_08830	GH77(13-487)	-	4-alpha-glucanotransferase
AArcSt11_09095	GT4(192-340)	-	GT
AArcSt11_09475	GH13(261-542)	-	alpha-amylase
AArcSt11_09505	GH13_31(35-378)	-	oligo-1,6-glucosidase
AArcSt11_09510	GH13_31(35-373)	-	oligo-1,6-glucosidase
AArcSt11_10040	GT66(34-675)	-	GT
AArcSt11_10245	GT2_Glycos_transf_2(9-188)	-	GT
AArcSt11_10395	GH31(169-598)	-	alpha-xylosidase
AArcSt11_10815	GH32(257-553)	-	beta-fructosidase
AArcSt11_10830	GH68(10-394)	-	beta-fructofuranosidase
AArcSt11_11000	GH81(77-713)	Tat/SPII	endo-1,3-beta-glucanase
AArcSt11_11010	GH3(90-311)	-	beta-xylosidase
AArcSt11_11550	GH2(562-966)	Tat/SPI	beta-galactosidase
AArcSt11_11555	GH2(11-816)	-	beta-galactosidase
AArcSt11_11560	GH42(6-385)	-	beta-galactosidase
AArcSt11_12085	GH2(20-555)	-	beta-mannosidase
AArcSt11_13975	GT2_Glycos_transf_2(4-150)	-	GT
AArcSt11_14230	GT81(99-289)	-	GT
AArcSt11_15975	GT4(185-321)	-	GT

Table S3: strain **AArc-St2**

Locus tag	**HMMER**	**Signal peptide** (SignalP v6.0)	**Function**
AArcSt2_00665	GT81(95-284)	-	GT
AArcSt2_00735	GT2_Glycos_transf_2(4-124)	-	GT
AArcSt2_00830	GT2_Glycos_transf_2(11-179)	-	GT
AArcSt2_01450	GH13_20(295-578)	-	alpha-amylase
AArcSt2_01455	GH15(289-664)	-	unknown
AArcSt2_04180	GH13_20(310-631)	Tat/SPI	alpha-amylase
AArcSt2_07575	GH32(257-554)	-	beta-fructosidase
AArcSt2_07580	GH68(24-404)	-	beta-fructofuranosidase
AArcSt2_07955	AA1(132-368)	Tat/SPII	multicopper oxidase MmcO
AArcSt2_08265	GH77(11-492)	-	4-alpha-glucanotransferase
AArcSt2_09525	GT4(179-315)	-	GT
AArcSt2_09610	AA7(38-407)	-	putative carbohydrate oxidase
AArcSt2_09745	GT81(20-200)	-	GT
AArcSt2_10530	GH13_31(35-392)	-	oligo-1,6-glucosidase
AArcSt2_10940	GT2_Glyco_tranf_2_3(5-221)	-	GT
AArcSt2_11025	GT4(197-341)	-	GT
AArcSt2_11040	GT4(188-339)	-	GT
AArcSt2_11045	GT4(195-343)	-	GT
AArcSt2_11300	GT2_Glycos_transf_2(4-168)	-	GT
AArcSt2_11305	GT66(41-730)	-	GT
AArcSt2_11675	GH37(27-499)	-	trehalase
AArcSt2_13715	GH16(26-261)	-	endo-1,3-1,4-beta-glucanase
AArcSt2_13720	GT2_Glyco_trans_2_3(103-297)	-	GT
AArcSt2_14250	GT2_Glycos_transf_2(9-182)	-	GT
AArcSt2_15130	AA7(36-407)	-	putative carbohydrate oxidase
AArcSt2_15190	PL1_2(117-291)	-	pectate lyase
AArcSt2_15275	GT4(211-360)	-	GT
AArcSt2_16150	GH13(285-569)	-	alpha-amylase
AArcSt2_16155	GH15(286-669)+GH15(1011-1402)	-	glucoamylase
AArcSt2_16605	GT4(182-322)	-	GT

Table S3: strain **AArc-dxtr1**

Locus tag	HMMER	Signal peptide (SignalP v6.0)	Function
OB905_00470	CBM57(258-374)+CBM57(461-571)	Sec/SPII	CBM
OB905_00495	CE14(8-117)	-	diacetylchitobiose deacetylase
OB905_00915	GH81(56-674)	Tat/SPI	endo-1,3(4)-beta-glucanase
OB905_01130	GH15(292-653)	-	trehalase
OB905_02070	CE14(8-117)	-	diacetylchitobiose deacetylase
OB905_02260	GT4(184-338)	-	GT
OB905_02685	GT2_Glycos_transf_2(9-191)	-	GT
OB905_02865	GT20(34-510)	-	GT
OB905_04265	CBM57(307-413)+CBM9(461-623)+CBM57(671-805)	Tat/SPII	CBM
OB905_04710	GT84(301-464)	Sec/SPII	GT
OB905_04715	CBM57(334-446)	Tat/SPII	CBM
OB905_04835	GT2_Glycos_transf_2(4-114)	-	GT
OB905_04890	GT81(105-288)	-	GT
OB905_05580	GT66(34-706)	-	GT
OB905_05585	GT2_Glycos_transf_2(4-168)	-	GT
OB905_05600	GT2_Glycos_transf_2(4-163)	-	GT
OB905_05605	GT2_Glycos_transf_2(16-178)	-	GT
OB905_05655	GT2_Glycos_transf_2(33-151)	-	GT
OB905_07190	GT4(226-380)	-	GT
OB905_07250	GH5(62-368)	Tat/SPI	endoglucanase
OB905_08350	GT2_Glyco_tranf_2_3(159-383)	-	GT
OB905_09375	CBM57(309-427)+CBM57(483-598)+CBM57(866-998)	Tat/SPII	CBM
OB905_10755	GT4(193-334)	-	GT
OB905_10845	GT4(163-311)	-	GT
OB905_10850	GT2_Glycos_transf_2(7-128)	-	GT
OB905_10865	GT4(207-364)	-	GT
OB905_10920	GT66(120-659)	-	GT
OB905_12615	CBM57(337-449)	Tat/SPII	CBM
OB905_12805	CBM57(339-442)	Tat/SPII	CBM
OB905_13355	CBM57(218-335)+CBM9(374-545)+CBM57(601-722)	Tat/SPII	CBM
OB905_13885	CBM57(320-442)+CBM57(457-602)	Tat/SPII	CBM

Table S3: AArc-curdl1

Locus tag	HMMER	Signal peptide (SignalP v6.0)	Function
OB919_00135	CBM34(8-130)+GH13_20(177-473)	-	neopullulanase
OB919_00155	GH15(317-728)	-	glucoamylase
OB919_00165	GH15(281-639)	-	unknown
OB919_00660	GT4(191-338)	-	GT
OB919_00740	AA7(36-408)	-	putative carbohydrate oxidase
OB919_00955	GH68(30-407)	-	beta-fructofuranosidase
OB919_01645	GT4(227-380)	-	GT
OB919_01700	GH2(3-594)	-	beta-mannosidase
OB919_02635	AA7(41-468)	-	putative carbohydrate oxidase
OB919_04360	CE14(4-113)	-	diacetylchitobiose deacetylase
OB919_04605	GH81(61-708)	Tat/SPI	endo-1,3(4)-beta-glucanase
OB919_04615	GH3(90-311)	-	beta-xylosidase
OB919_04770	GH2(15-502)	-	beta-galactosidase
OB919_04790	GH5_13(34-294)	-	unknown
OB919_04795	GH2(4-751)	-	beta-galactosidase
OB919_04935	AA7(34-458)	-	putative carbohydrate oxidase
OB919_05150	AA7(34-460)	-	putative carbohydrate oxidase
OB919_07805	GH13(353-689)+CBM13(856-996)	Tat/SPI	alpha-amylase
OB919_09760	CE1(46-225)	-	probable carboxylesterase
OB919_09840	GT81(107-296)	-	GT
OB919_10890	GT2_Glycos_transf_2(5-114)	-	GT
OB919_11965	GH13(238-521)	-	alpha-amylase
OB919_11970	GH15(277-653)+GH15(995-1386)	-	glucoamylase
OB919_11975	GH77(15-494)	-	4-alpha-glucanotransferase
OB919_12000	GH32(296-592)	-	beta-fructosidase
OB919_12295	GT4(186-327)	-	GT
OB919_12310	GT4(202-351)	-	GT
OB919_12920	GH15(235-593)	-	trehalase
OB919_13510	GH73(562-672)	Tat/SPI	putative murein hydrolase
OB919_13880	GT2_Glycos_transf_2(10-130)	-	GT
OB919_13890	GT2_Glycos_transf_2(6-170)	-	GT
OB919_13895	GT66(33-673)	-	GT
OB919_15140	CE4(224-348)	Sec/SPII or Tat/	unknown
OB919_17020	GT4(106-256)	-	GT
OB919_17040	CE4(60-190)	-	peptidoglycan deacetylase
OB919_17180	GT2_Glycos_transf_2(9-196)	-	GT
OB919_17185	CE4(48-162)	-	peptidoglycan deacetylase
OB919_18290	GT2_Glycos_transf_2(49-165)	-	GT
OB919_18550	GT20(41-529)	-	GT
OB919_19885	GH36(56-504)	-	alpha-galactosidase
OB919_19890	GH42(6-390)	-	beta-galactosidase
OB919_20390	GH13(305-655)	Tat/SPI	alpha-amylase
OB919_20490	AA7(33-404)	-	putative carbohydrate oxidase
OB919_20920	GT4(191-340)	-	GT

Table S3: strain **AArc-xg1-1**

Locus tag	HMMER	Signal peptide (SignalP v6.0)	Function
OB960_00040	GT4(184-320)	-	GT
OB960_00055	GT4(219-369)	-	GT
OB960_00060	GT2_Glycos_transf_2(4-168)	-	GT
OB960_00065	GT66(35-696)	-	GT
OB960_00460	GH15(248-609)	-	trehalase
OB960_01395	GT4(196-338)	-	GT
OB960_01410	GT4(202-350)	-	GT
OB960_02060	GH13_20(292-595)	-	alpha-amylase
OB960_02065	GH15(283-639)	-	glucoamylase
OB960_02575	GH105(40-342)	-	Unsaturated rhamnogalacturonyl hydrolase
OB960_02700	AA7(38-471)	-	putative carbohydrate oxidase
OB960_03335	GH3(52-260)	-	beta-glucosidase
OB960_04290	GH5(65-356)+CBM6(517-657)	Tat/SPI	endoglucanase
OB960_04295	GH5_7(92-386)	Tat/SPI	endo-1,4-beta-mannosidase
OB960_04300	GH5_7(96-387)	Tat/SPI	endo-1,4-beta-mannosidase
OB960_04315	GH5(66-371)	Tat/SPI	endoglucanase
OB960_04320	PL14_3(113-318)	Tat/SPI	unknown
OB960_04325	GH5(87-390)	Tat/SPI	endoglucanase
OB960_04340	GH5(97-403)	Tat/SPI	endoglucanase
OB960_04345	GH10(118-438)	Tat/SPI	celloxylanase/endo-1,4-beta-xylanase
OB960_04350	GH10(121-457)	Tat/SPI	endo-1,4-beta-xylanase
OB960_04355	GH10(117-443)	Tat/SPI	endo-1,4-beta-xylanase
OB960_04360	GH5(46-494)	Sec/SPI	endoglucanase
OB960_04365	GH5_7(108-396)	Tat/SPI	endo-1,4-beta-mannosidase
OB960_04375	GH5(68-392)	Tat/SPI	endoglucanase
OB960_04380	GH5(64-464)	Tat/SPI	endoglucanase
OB960_04385	GH5(84-402)	Tat/SPI	endoglucanase
OB960_04680	GT4(201-341)	-	GT
OB960_05170	GH3(90-314)	-	beta-glucosidase
OB960_05540	GH43_3(46-348)	Tat/SPI	exo-alpha-1,5-L-arabinofuranosidase
OB960_05580	AA7(34-458)	-	putative carbohydrate oxidase
OB960_06075	GH9(142-643)	Tat/SPI	endoglucanase
OB960_06245	GH43_12(5-284)	-	alpha-L-arabinofuranosidase
OB960_06735	PL1_2(110-300)	Tat/SPI	pectate lyase
OB960_06740	PL1_2(109-280)	Tat/SPI	pectate lyase
OB960_06875	GT87(71-307)	Sec/SPI or no	GT
OB960_06900	GH109(3-151)	-	D-glucoside 3-dehydrogenase
OB960_07565	GH145(28-333)	-	alpha-L-rhamnosidase
OB960_07570	GH42(6-387)	-	beta-galactosidase
OB960_07700	GH11(19-153)+CBM13(199-287	-	endo-1,4-beta-xylanase
OB960_07770	CBM85(41-175)	-	CBM
OB960_07965	GT20(10-480)	-	GT
OB960_08965	GH93(28-377)	-	exo-alpha-L-1,5-arabinanase
OB960_09825	GT2_Glycos_transf_2(5-114)	-	GT
OB960_10920	GH2(22-579)	-	beta-mannosidase
OB960_11235	GT2_Glycos_transf_2(9-175)	-	GT
OB960_11335	GT2_Glyco_tranf_2_3(87-303)	-	GT
OB960_11390	GH4(3-181)	-	alpha-galactosidase
OB960_12685	GH11(34-200)	Sec/SPI	endo-1,4-beta-xylanase
OB960_13415	PL11(1-588)	-	rhamnogalacturonan lyase
OB960_13425	GH43_18(45-275)	-	endo-1,5-alpha-L-arabinosidase
OB960_13430	GH95(7-795)	-	alpha-L-fucosidase
OB960_13460	PL22(44-149)+PL22(190-392)	-	oligogalacturonide lyase
OB960_13470	GH106(13-773)	-	unknown
OB960_13475	GH51(229-726)	-	alpha-L-arabinofuranosidase
OB960_13490	CBM67(119-302)+GH78(322-85	-	alpha-L-rhamnosidase
OB960_13505	PL22(44-149)+PL22_2(180-374	-	oligogalacturonide lyase
OB960_13510	PL22_2(188-380)	-	oligogalacturonide lyase
OB960_13610	GH28(63-446)	-	polygalacturonase
OB960_13635	PL26(6-867)	-	rhamnogalacturonan exolyase
OB960_13640	GH2(5-701)	-	beta-glucuronidase
OB960_13650	GH2(60-833)	Tat/SPI	beta-galactosidase
OB960_13655	CBM13(565-705)	Tat/SPI	CBM
OB960_13815	PL1_2(529-716)	Tat/SPI	pectate lyase
OB960_13825	PL1_2(909-1102)	Tat/SPI	pectate lyase
OB960_13895	GH28(33-390)	-	polygalacturonase
OB960_14045	GH127(15-550)	-	beta-L-arabinofuranosidase
OB960_14065	GH2(9-665)	-	beta-glucuronidase
OB960_14095	GH43_3(32-328)	Tat/SPII	endo-alpha-1,5-L-arabinanase
OB960_14110	GH2(8-471)	-	beta-glucuronidase
OB960_14115	GH51(3-499)	-	alpha-L-arabinofuranosidase
OB960_14315	GH28(29-392)	-	polygalacturonase
OB960_14320	PL22(40-152)+PL22_2(203-381	-	oligogalacturonide lyase
OB960_14325	CBM9(17-222)	-	CBM
OB960_14330	GH115(20-717)	-	alpha-1,2-glucuronidase
OB960_14340	GH4(20-200)	-	alpha-galacturonidase
OB960_14355	CBM67(358-531)+GH78(560-10	-	alpha-L-rhamnosidase
OB960_14360	CBM13(589-723)	Tat/SPI	CBM
OB960_14620	GH2(5-579)	-	beta-glucuronidase
OB960_14635	GH5(59-331)+CBM9(484-651)	Tat/SPII	endoglucanase
OB960_14745	GT4(180-276)	-	GT
OB960_14810	GT2_Glycos_transf_2(5-110)	-	GT
OB960_15085	GH2(36-945)	-	beta-galactosidase
OB960_15125	CE4(226-344)	Tat/SPII	polysaccharide deacetylase
OB960_15330	GT20(82-541)	-	GT
OB960_15510	GT2_Glyco_tranf_2_3(60-325)	-	GT
OB960_15565	CE4(3-135)	-	peptidoglycan deacetylase
OB960_15600	GT4(195-350)	-	GT
OB960_15620	GT2_Glycos_transf_2(5-113)	-	GT
OB960_15625	GT4(218-370)	-	GT
OB960_16100	GT2_Glycos_transf_2(18-156)	-	GT
OB960_16385	CE4(219-337)	Tat/SPII	putative polysaccharide deacetylase
OB960_16590	CE14(4-113)	-	diacetylchitobiose deacetylase
OB960_16665	CE14(17-126)	-	diacetylchitobiose deacetylase
OB960_16820	GH32(24-329)	-	beta-fructosidase
OB960_16825	GH154(11-359)	-	putative beta-glucuronidase
OB960_17195	GH31(221-716)	-	alpha-xylosidase
OB960_17200	GH5(67-371)	Tat/SPI	endoglucanase
OB960_17950	CE14(6-115)	-	diacetylchitobiose deacetylase
OB960_18050	CE15(84-403)+CE15(442-766)	-	4-O-methyl-glucuronoyl methylesterase
OB960_18060	PL40(597-926)	-	putative ulvan lyase
OB960_18145	CE14(9-118)	-	diacetylchitobiose deacetylase
OB960_18930	PL25(2-133)	-	ulvan lyase
OB960_19135	GT2_Glycos_transf_2(33-178)	-	GT
OB960_19520	GT4(204-342)	-	GT
OB960_19530	GT4(195-345)	-	GT
OB960_19545	GT4(181-331)	-	GT
OB960_19580	GT2_Glycos_transf_2(70-230)	-	GT
OB960_19595	CE15(19-396)	-	carbohydrate esterase
OB960_20140	GT4(226-382)	-	GT
OB960_20475	GH3(43-254)	-	beta-glucosidase
OB960_20885	GH43_12(5-279)	-	alpha-L-arabinofuranosidase
OB960_20890	GH159(23-239)	-	beta-D-galactofuranosidase
OB960_21020	GT2_Glyco_tranf_2_3(46-263)	-	GT
OB960_21120	GH4(3-181)	-	alpha-galactosidase
OB960_21555	GH2(41-943)	-	beta-galactosidase
OB960_21560	GH2(36-930)	-	beta-galactosidase
OB960_21575	GH145(28-311)	-	aplha-L-rhamnosidase
OB960_21580	GH30_4(135-587)	-	endo-beta-1,6-galactanase
OB960_21645	GH2(54-645)	Sec/SPII or Sec/	beta-glucuronidase
OB960_21710	GH88(44-379)	-	unsaturated glucuronyl hydrolase
OB960_21830	GH95(8-739)	-	alpha-L-fucosidase
OB960_21835	GH29(3-348)	-	alpha-L-fucosidase
OB960_21920	GH3(86-315)	-	beta-xylosidase
OB960_22090	GH2(3-711)	-	beta-mannosidase
OB960_22105	GH5_8(96-291)	Tat/SPI	endo-1,4-beta-mannosidase
OB960_22110	GH43_3(44-331)+CBM13(361-5	Tat/SPI	endo-alpha-1,5-L-arabinanase
OB960_22120	GH26(67-364)	Tat/SPI	endo-1,4-beta-mannosidase
OB960_22140	GH5_7(89-381)	Tat/SPII	endo-1,4-beta-mannosidase
OB960_23595	GH29(4-360)	-	alpha-L-fucosidase
OB960_23605	GH29(15-352)	-	alpha-L-fucosidase
OB960_23610	GH29(4-348)	-	alpha-L-fucosidase
OB960_23615	GH29(8-315)	-	alpha-L-fucosidase
OB960_24985	CBM67(325-482)+GH78(544-10	-	alpha-L-rhamnosidase
OB960_24990	GH2(6-568)	-	beta-glucuronidase
OB960_25000	GH2(2-507)	-	beta-galactosidase
OB960_25020	GH42(25-404)	-	beta-galactosidase
OB960_25025	CBM13(418-510)	Tat/SPI	CBM
OB960_25065	GH29(3-373)	-	alpha-L-fucosidase
OB960_25070	GH29(5-351)	-	alpha-L-fucosidase
OB960_25175	GH10(8-318)	-	endo-1,4-beta-xylanase
OB960_25180	GH4(29-206)	-	alpha-galacturonidase
OB960_25190	GH3(66-292)	-	beta-xylosidase
OB960_25225	GH67(8-688)	-	alpha-glucuronidase
OB960_25230	CBM85(106-238)+CBM85(329-4	Tat/SPI	endo-1,4-beta-xylanase
OB960_25235	CBM6(2-87)	-	CBM
OB960_25580	GH29(3-299)	-	alpha-L-fucosidase
OB960_25600	GH95(7-734)	-	alpha-L-fucosidase
OB960_25715	GH51(289-807)	Tat/SPII	alpha-1,5-L-arabinofuranosidase

Table S3: strain **AArc-m2/3/4**

Locus tag	HMMER	Signal peptide (SignalP v6.0)	Function
OB955_01610	GH3(52-260)	-	beta-glucosidase
OB955_02250	AA7(38-471)	-	putative carbohydrate oxidase
OB955_02375	GH105(40-342)	-	unsaturated rhamnogalacturonyl hydrolase
OB955_02890	GH15(283-639)	-	unknown
OB955_02895	GH13_20(292-598)	-	alpha-amylase
OB955_03545	GT4(202-350)	-	GT
OB955_03560	GT4(196-338)	-	GT
OB955_04535	GH11(34-200)	Sec/SPI	endo-1,4-beta-xylanase
OB955_05955	GH5(67-371)	Tat/SPI	endoglucanase
OB955_05960	GH31(221-716)	-	alpha-xylosidase
OB955_06040	GH11(76-245)+CBM13(291-380)+CBM13(358-426)	Tat/SPI	endo-1,4-beta-xylanase
OB955_06045	CBM6(2-87)	-	CBM
OB955_06050	CBM85(106-238)+CBM85(329-460)+GH10(518-835)	Tat/SPI	endo-1,4-beta-xylanase
OB955_06055	GH67(8-688)	-	alpha-1,2-glucuronosidase
OB955_06090	GH3(66-292)	-	beta-xylosidase
OB955_06100	GH4(29-206)	-	alpha-galacturonidase
OB955_06105	GH10(8-318)	-	endo-1,4-beta-xylanase
OB955_06205	GH42(6-387)	-	beta-galactosidase
OB955_06210	GH145(28-333)	-	aplha-L-rhamnosidase
OB955_06740	GH109(3-151)	-	D-glucoside 3-dehydrogenase
OB955_06765	GT87(71-307)	Sec/SPI	GT
OB955_06995	AA7(34-458)	-	putative carbohydrate oxidase
OB955_07035	GH43_3(46-348)	Tat/SPI	endo-alpha-1,5-L-arabinanase
OB955_07405	GH3(90-314)	-	beta-glucosidase
OB955_07895	GT4(201-341)	-	GT
OB955_08185	GH5(84-402)	Tat/SPI	endoglucanase
OB955_08190	GH5(64-464)	Tat/SPI	endoglucanase
OB955_08195	GH5(68-392)	Tat/SPI	endoglucanase
OB955_08205	GH5_7(108-396)	Tat/SPI	endo-1,4-beta-mannosidase
OB955_08210	GH5(46-494)	Sec/SPI	endoglucanase
OB955_08215	GH10(117-443)	Tat/SPI	endo-1,4-beta-xylanase
OB955_08220	GH10(121-461)	Tat/SPI	endo-1,4-beta-xylanase
OB955_08225	GH10(118-438)	Tat/SPI	celloxylanase/endo-1,4-beta-xylanase
OB955_08230	GH5(97-403)	Tat/SPI	endoglucanase
OB955_08245	GH5(87-390)	Tat/SPI	endoglucanase
OB955_08250	PL14_3(113-318)	Tat/SPI	unknown
OB955_08255	GH5(66-371)	Tat/SPI	endoglucanase
OB955_08270	GH5_7(64-354)	Sec/SPI	endo-1,4-beta-mannosidase
OB955_08275	GH5_7(92-386)	Tat/SPI	endo-1,4-beta-mannosidase
OB955_08280	GH5(65-356)+CBM6(517-657)	Tat/SPI	endoglucanase
OB955_09465	GH109(3-365)	-	alpha-N-acetylgalactosaminidase
OB955_09620	GT2_Glycos_transf_2(33-178)	-	GT
OB955_09650	GT2_Glycos_transf_2(4-166)	-	GT
OB955_09655	GT2_Glycos_transf_2(4-168)	-	GT
OB955_09660	GT66(35-696)	-	GT
OB955_10060	GH15(248-609)	-	trehalase
OB955_10930	GH93(28-377)	-	alpha-L-arabinofuranobiosidase
OB955_11765	GH51(3-499)	-	alpha-L-arabinofuranosidase
OB955_11770	GH2(8-471)	-	beta-glucuronidase
OB955_11785	GH43_3(32-328)	Tat/SPII	endo-alpha-1,5-L-arabinanase
OB955_11815	GH2(9-667)	-	beta-glucuronidase
OB955_11835	GH127(15-550)	-	beta-L-arabinofuranosidase
OB955_11990	GH28(33-390)	-	polygalacturonase
OB955_12060	PL1_2(1108-1301)	Tat/SPI	pectate lyase
OB955_12070	PL1_2(529-716)	Tat/SPI	pectate lyase
OB955_12230	CBM13(565-705)	Tat/SPI	CBM
OB955_12235	GH2(60-833)	Tat/SPI	beta-galactosidase
OB955_12245	GH2(5-482)	-	beta-glucuronidase
OB955_12250	PL26(6-867)	-	rhamnogalacturonan exolyase
OB955_12275	GH28(63-446)	-	polygalacturonase
OB955_12375	PL22_2(188-380)	-	oligogalacturonate lyase
OB955_12380	PL22(44-149)+PL22_2(180-374)	-	oligogalacturonide lyase
OB955_12395	CBM67(119-302)+GH78(322-852)	-	alpha-L-rhamnosidase
OB955_12410	GH51(230-726)	-	alpha-L-arabinofuranosidase
OB955_12415	GH106(13-765)	-	putative alpha-L-rhamnosidase
OB955_12425	PL22(46-151)+PL22(192-394)	-	oligogalacturonide lyase
OB955_12455	GH95(7-795)	-	alpha-L-fucosidase
OB955_12460	GH43_18(45-275)	-	putative endo-1,5-alpha-L-arabinosidase
OB955_12470	PL11(1-588)	-	rhamnogalacturonan lyase
OB955_12485	CBM67(325-482)+GH78(544-1065)	-	alpha-L-rhamnosidase
OB955_12490	GH2(6-568)	-	beta-glucuronidase
OB955_12500	GH2(2-507)	-	beta-galactosidase
OB955_12520	GH42(25-404)	-	beta-galactosidase
OB955_12525	CBM13(418-510)+CBM13(487-557)	Tat/SPI	CBM
OB955_12630	PL1_2(109-280)	Tat/SPI	pectate lyase
OB955_12635	PL1_2(110-300)	Tat/SPI	pectate lyase
OB955_13125	GH43_12(5-284)	-	alpha-L-arabinofuranosidase
OB955_13295	GH9(142-643)	Tat/SPI	endoglucanase
OB955_13755	CE14(4-113)	-	diacetylchitobiose deacetylase
OB955_13830	CE14(17-126)	-	diacetylchitobiose deacetylase
OB955_13985	GH32(24-329)	-	beta-fructosidase
OB955_13990	GH154(11-359)	-	putative beta-glucuronidase
OB955_15065	GH2(41-943)	-	beta-galactosidase
OB955_15075	GH2(36-930)	-	beta-galactosidase
OB955_15090	GH145(28-311)	-	alpha-L-rhamnosidase
OB955_15095	GH30_4(135-587)	-	endo-beta-1,6-galactanase
OB955_15160	GH2(54-645)	Sec/SPII or Sec/S	beta-glucuronidase
OB955_15220	GH88(44-378)	-	unsaturated glucuronyl hydrolase
OB955_15340	GH95(8-739)	-	alpha-L-fucosidase
OB955_15345	GH29(3-348)	-	alpha-L-fucosidase
OB955_15370	GH2(5-579)	-	beta-galactosidase
OB955_15385	GH5(59-331)+CBM9(484-651)	Tat/SPII	endoglucanase
OB955_15495	GT4(180-276)	-	GT
OB955_15565	GT2_Glycos_transf_2(5-109)	-	GT
OB955_15825	GH2(36-945)	-	beta-galactosidase
OB955_15865	CE4(226-344)	Tat/SPII	putative polysaccharide deacetylase
OB955_16070	GT20(87-541)	-	GT
OB955_16185	GH3(43-254)	-	beta-glucosidase
OB955_16595	GH43_12(5-279)	-	alpha-L-arabinofuranosidase
OB955_16600	GH159(23-239)	-	putative beta-D-galactofuranosidase
OB955_16830	GH4(3-181)	-	alpha-galactosidase
OB955_17315	GT2_Glycos_transf_2(5-115)	-	GT
OB955_18455	CE4(219-337)	Tat/SPII	putative polysaccharide deacetylase
OB955_18740	GT2_Glycos_transf_2(18-156)	-	GT
OB955_19385	GT4(204-342)	-	GT
OB955_19395	GT4(195-345)	-	GT
OB955_19405	GT4(179-331)	-	GT
OB955_19435	GT2_Glycos_transf_2(62-222)	-	GT
OB955_19450	CE15(19-396)	-	carbohydrate esterase
OB955_19975	GT8(1-224)	-	GT
OB955_19980	GT2_Glycos_transf_2(9-154)	-	GT
OB955_19985	GT4(202-343)	-	GT
OB955_20065	GT4(200-341)	-	GT
OB955_20370	GH4(3-181)	-	alpha-galactosidase
OB955_20515	GT2_Glycos_transf_2(9-175)	-	GT
OB955_20830	GH2(22-579)	-	beta-mannosidase
OB955_21395	GH51(290-806)	Tat/SPII	alpha-1,5-L-arabinofuranosidase
OB955_21595	GH28(29-392)	-	polygalacturonase
OB955_21600	PL22(40-152)+PL22_2(203-381)	-	oligogalacturonide lyase
OB955_21605	CBM9(17-222)	-	CBM
OB955_21610	GH115(21-728)	-	alpha-glucuronidase
OB955_21620	GH4(20-200)	-	alpha-galacturonidase
OB955_21635	CBM67(359-507)+GH78(567-1080)	-	alpha-L-rhamnosidase
OB955_21640	CBM13(589-723)	Tat/SPI	CBM
OB955_21990	GT2_Glycos_transf_2(141-292)	-	GT
OB955_21995	GT2_Glycos_transf_2(52-178)	-	GT
OB955_22025	GT2_Glycos_transf_2(22-144)	-	GT
OB955_22425	GH88(40-374)	-	unsaturated glucuronyl hydrolase
OB955_22455	GH29(2-352)	-	alpha-L-fucosidase
OB955_22465	GH137(47-345)	-	putative beta-L-arabinofuranosidase
OB955_22485	GH2(29-582)+GH2(808-1117)	-	beta-galactosidase
OB955_22490	GH2(30-696)	-	beta-galactosidase
OB955_22525	GH29(3-339)	-	alpha-L-fucosidase
OB955_22530	GH2(31-818)	-	beta-galactosidase
OB955_22540	GH29(13-380)	-	alpha-L-fucosidase
OB955_22590	CBM67(114-298)+GH78(320-840)	-	alpha-L-rhamnosidase
OB955_22595	GH106(12-746)	-	alpha-L rhamnosidase
OB955_22610	CBM67(339-504)+GH78(530-1037)	-	alpha-L-rhamnosidase
OB955_22620	GH33(23-339)	-	putative sialidase
OB955_22640	CBM67(141-307)+GH78(331-838)	-	alpha-L-rhamnosidase
OB955_22770	GH5_7(89-381)	Tat/SPII	endo-1,4-beta-mannosidase
OB955_22790	GH26(67-364)	Tat/SPI	endo-1,4-beta-mannosidase
OB955_22795	GH43_3(44-331)+CBM13(361-502)	Tat/SPI	endo-alpha-1,5-L-arabinanase
OB955_22800	GH5_8(96-291)	Tat/SPI	endo-1,4-beta-mannosidase
OB955_22815	GH2(3-691)	-	beta-mannosidase
OB955_22985	GH3(86-315)	-	beta-xylosidase
OB955_23495	GT20(10-480)	-	GT
OB955_23685	CBM85(71-205)	-	CBM
OB955_24005	GT2_Glyco_tranf_2_3(87-303)	-	GT
OB955_24060	GH4(3-181)	-	alpha-galactosidase
OB955_24200	GH95(7-734)	-	alpha-L-fucosidase
OB955_24390	GT4(225-382)	-	GT
OB955_25125	GH29(8-315)	-	alpha-L-fucosidase
OB955_25130	GH29(4-348)	-	alpha-L-fucosidase
OB955_25135	GH29(15-352)	-	alpha-L-fucosidase
OB955_25145	GH29(4-360)	-	alpha-L-fucosidase
OB955_25560	GH29(5-351)	-	alpha-L-fucosidase
OB955_25565	GH29(3-174)	-	alpha-L-fucosidase
OB955_25600	GH29(15-209)	-	alpha-L-fucosidase

Table S3: strain **HArc-curdl5-1**

Locus tag	**HMMER**	**Signal peptide** (SignalP v6.0)	**Function**
OB916_00345	GH15(314-667)	-	glucoamylase
OB916_00405	GH13_20(277-566)	-	alpha-amylase
OB916_00500	GH13(281-595)	-	alpha-amylase
OB916_01050	GH2(17-600)	-	exo-beta-D-glucosaminidase
OB916_01685	GH13(285-575)	-	alpha-amylase
OB916_01715	GH13_31(28-393)	-	oligo-1,6-glucosidase
OB916_02035	GH13(305-685)	Tat/SPI	alpha-amylase
OB916_02345	GT4(186-297)	-	GT
OB916_02400	GT75(87-370)	-	GT
OB916_02430	GT2_Glycos_transf_2(10-165)	-	GT
OB916_02715	GH13_4(114-512)+CBM20(663-734)	-	amylosucrase
OB916_02720	GH13_16(30-385)	-	trehalose synthase/amylase
OB916_02730	GH13_31(28-371)	-	oligo-1,6-glucosidase
OB916_02740	GH13_31(39-384)	-	oligo-1,6-glucosidase
OB916_03150	GH81(63-741)+CBM6(1032-1168)	Tat/SPI	endo-1,3(4)-beta-glucanase
OB916_03200	GH3(95-321)	-	beta-xylosidase
OB916_03355	GT81(6-185)	-	GT
OB916_03680	GH15(300-664)	-	unknown
OB916_03740	GH77(11-490)	-	4-alpha-glucanotransferase
OB916_03760	GH13(253-531)	-	alpha-amylase
OB916_03765	GT35(173-517)	-	glycogen phosphorylase
OB916_04015	GH13_16(30-383)	-	trehalose synthase/amylase
OB916_04285	GH13_20(292-570)	Tat/SPI	alpha-amylase
OB916_04550	GH13(280-595)	-	alpha-amylase
OB916_05655	GT81(99-284)	-	GT
OB916_06405	GT2_Glycos_transf_2(36-148)	-	GT
OB916_06415	CE4(31-142)	-	peptidoglycan deacetylase
OB916_06515	GH13(17-327)	-	alpha-amylase
OB916_07025	GH13(321-613)	Tat/SPII	alpha-amylase
OB916_07685	GT2_Glycos_transf_2(5-122)	-	GT
OB916_08130	GT4(178-321)	-	GT
OB916_08575	GH15(321-671)	-	glucoamylase
OB916_08850	GT66(123-614)	-	GT
OB916_08935	GT66(32-522)	-	GT
OB916_09025	GH31(172-599)	-	alpha-xylosidase
OB916_09030	GH31(170-597)	-	alpha-xylosidase
OB916_09050	GT2_Glycos_transf_2(39-200)	-	GT
OB916_09055	GT4(213-346)	-	GT
OB916_09065	GT4(202-335)	-	GT
OB916_09090	GT4(199-342)	-	GT
OB916_09325	GT2_Glycos_transf_2(8-174)	-	GT
OB916_10135	GT87(72-225)	-	GT
OB916_10280	GT66(31-651)	-	GT
OB916_10285	GT2_Glycos_transf_2(5-173)	-	GT
OB916_10290	GT4(204-325)	-	GT
OB916_10305	GT4(204-312)	-	GT
OB916_10350	GH13(59-326)	-	alpha-amylase
OB916_10585	GT2_Glyco_trans_2_3(173-363)	-	GT
OB916_10690	GH42(6-387)	-	beta-galactosidase
OB916_10715	GH27(109-368)	-	alpha-galactosidase
OB916_10720	GH4(4-181)	-	alpha-galactosidase
OB916_10745	GH13_20(295-633)	-	alpha-amylase
OB916_11155	GT2_Glycos_transf_2(9-192)	-	GT
OB916_12495	GT35(171-488)	-	glycogen phosphorylase
OB916_12725	GH13_32(48-280)	-	alpha-amylase
OB916_13250	GH37(27-505)	-	trehalase
OB916_14480	AA7(41-340)	-	putative carbohydrate oxidase
OB916_15020	GT4(191-313)	-	GT
OB916_15420	GT4(182-323)	-	GT
OB916_15425	GT4(200-338)	-	GT
OB916_15735	GH3(40-248)	-	beta-glucosidase
OB916_16085	GT83(139-434)	-	GT
OB916_16280	GT4(151-301)	-	GT
OB916_16390	GT2_Glycos_transf_2(11-170)	-	GT
OB916_16405	GT4(187-327)	-	GT
OB916_16440	GT4(191-324)	-	GT
OB916_16495	AA7(35-461)	-	putative carbohydrate oxidase
OB916_16585	GH161(1-1060)	-	beta-1,3-glucan phosphorylase

Table S3: strain **HArc-curdl7**

Locus tag	**HMMER**	**Signal peptide** (SignalP v6.0)	**Function**
OB914_00280	GH13_31(39-384)	-	oligo-1,6-glucosidase
OB914_00290	GH13_31(28-371)	-	oligo-1,6-glucosidase
OB914_00300	GH13_16(30-385)	-	trehalose synthase/amylase
OB914_00305	GH13_4(114-512)+CBM20(663-734)	-	amylosucrase
OB914_00590	GT2_Glycos_transf_2(10-165)	-	GT
OB914_00620	GT75(87-370)	-	GT
OB914_00675	GT4(186-297)	-	GT
OB914_00985	GH13(305-685)	Tat/SPI	alpha-amylase
OB914_01305	GH13_31(28-393)	-	oligo-1,6-glucosidase
OB914_01335	GH13(285-575)	-	alpha-amylase
OB914_01970	GH2(17-600)	-	exo-beta-D-glucosaminidase
OB914_02520	GH13(281-595)	-	alpha-amylase
OB914_02615	GH13_20(277-566)	-	alpha-amylase
OB914_02675	GH15(314-667)	-	glucoamylase
OB914_03085	GH161(1-1060)	-	beta-1,3-glucan phosphorylase
OB914_03225	GH81(55-733)+CBM6(1024-1160)	Tat/SPI	endo-1,3(4)-beta-glucanase
OB914_03275	GH3(95-321)	-	beta-xylosidase
OB914_03430	GT81(6-185)	-	GT
OB914_03755	GH15(300-664)	-	unknown
OB914_03815	GH77(11-490)	-	4-alpha-glucanotransferase
OB914_03835	GH13(253-531)	-	alpha-amylase
OB914_03840	GT35(173-517)	-	glycogen phosphorylase
OB914_04090	GH13_16(30-383)	-	trehalose synthase/amylase
OB914_04360	GH13_20(292-570)	Tat/SPI	alpha-amylase
OB914_04625	GH13(280-595)	-	alpha-amylase
OB914_05085	GT4(199-342)	-	GT
OB914_05110	GT4(202-335)	-	GT
OB914_05120	GT4(213-346)	-	GT
OB914_05125	GT2_Glycos_transf_2(39-200)	-	GT
OB914_05145	GH31(170-597)	-	alpha-xylosidase
OB914_05150	GH31(172-599)	-	alpha-xylosidase
OB914_05240	GT66(32-522)	-	GT
OB914_05445	GT66(123-614)	-	GT
OB914_05585	GT4(204-312)	-	GT
OB914_05600	GT4(204-325)	-	GT
OB914_05605	GT2_Glycos_transf_2(5-173)	-	GT
OB914_05610	GT66(31-651)	-	GT
OB914_05755	GT87(72-225)	-	GT
OB914_06990	GT81(99-284)	-	GT
OB914_07210	GH13(17-327)	-	alpha-amylase
OB914_07310	CE4(31-142)	-	peptidoglycan deacetylase
OB914_07320	GT2_Glycos_transf_2(36-148)	-	GT
OB914_08360	GH13(321-613)	Tat/SPII	alpha-amylase
OB914_09025	GT2_Glycos_transf_2(5-122)	-	GT
OB914_09475	GT4(6-149)	-	GT
OB914_09955	GT2_Glycos_transf_2(8-174)	-	GT
OB914_10385	GH15(321-671)	-	glucoamylase
OB914_10740	GH13_20(295-633)	-	alpha-amylase
OB914_10765	GH4(4-181)	-	alpha-galactosidase
OB914_10770	GH27(109-368)	-	alpha-galactosidase
OB914_10795	GH42(6-387)	-	beta-galactosidase
OB914_10900	GT2_Glyco_trans_2_3(173-363)	-	GT
OB914_11135	GH13(72-339)	-	alpha-amylase
OB914_11200	GT2_Glycos_transf_2(9-192)	-	GT
OB914_12880	GT35(171-488)	-	glycogen phosphorylase
OB914_13365	GH37(27-505)	-	trehalase
OB914_13620	GH13_32(48-280)	-	alpha-amylase
OB914_14180	GT4(151-301)	-	GT
OB914_15255	AA7(41-340)	-	putative carbohydrate oxidase
OB914_15565	GT4(191-313)	-	GT
OB914_15955	GT4(182-323)	-	GT
OB914_15960	GT4(200-338)	-	GT
OB914_16065	GH3(53-261)	-	beta-glucosidase
OB914_16185	GT83(139-434)	-	GT
OB914_16330	GT4(191-324)	-	GT
OB914_16365	GT4(187-327)	-	GT
OB914_16380	GT2_Glycos_transf_2(11-170)	-	GT
OB914_16575	AA7(35-461)	-	putative carbohydrate oxidase

Table S3: strain **HArc-gm2**

Locus tag	**HMMER**	**Signal peptide** (SignalP v6.0)	**Function**
OB920_01505	GT4(181-321)	-	GT
OB920_01510	GT4(198-337)	-	GT
OB920_01535	GH3(40-247)	-	beta-glucosidase
OB920_03705	GT81(4-188)	-	GT
OB920_03720	GT4(206-339)	-	GT
OB920_03755	GT4(208-354)	-	GT
OB920_03760	GT2_Glycos_transf_2(7-121)	-	GT
OB920_03765	GT66(35-658)	-	GT
OB920_05495	GH3(80-307)	-	beta-xylosidase
OB920_06225	GH5(69-384)	Tat/SPI	endoglucanase
OB920_06230	GH5(63-434)	Tat/SPI	endoglucanase
OB920_06240	CE6(131-235)+CBM6(362-498)	Tat/SPI	carbohydrate acetyl esterase/feruloyl esterase
OB920_06250	GH5(82-366)+CBM6(521-656)	Tat/SPI	endoglucanase
OB920_06255	GH10(108-434)	Tat/SPI	endo-1,4-beta-xylanase
OB920_06260	GH5(84-385)	Tat/SPI	endoglucanase
OB920_06590	GH10(12-319)	-	endo-1,4-beta-xylanase
OB920_06600	GH4(19-195)	-	alpha-galacturonidase
OB920_06605	CBM85(93-228)+GH10(294-596)	Tat/SPI	endo-1,4-beta-xylanase
OB920_07170	GH3(89-316)	-	beta glucosidase
OB920_07405	GH2(19-368)	-	beta-mannosidase
OB920_07500	CBM85(91-226)+GH10(287-588)	Tat/SPI	endo-1,4-beta-xylanase
OB920_08310	GT4(194-342)	-	GT
OB920_08320	GT4(215-375)	-	GT
OB920_08325	GT2_Glycos_transf_2(5-162)	-	GT
OB920_08345	GT4(190-350)	-	GT
OB920_08395	GT66(112-597)	-	GT
OB920_08980	CBM6(72-171)	-	CBM
OB920_09185	GH4(3-181)	-	alpha-galactosidase
OB920_09195	GH4(3-180)	-	alpha-galactosidase
OB920_09210	GH2(29-934)	-	beta-galactosidase
OB920_09290	GH43_3(45-346)+CBM13(399-535)	Tat/SPI	endo-alpha-1,5-L-arabinanase
OB920_09435	GT2_Glycos_transf_2(9-162)	-	GT
OB920_09470	GT2_Glycos_transf_2(5-114)	-	GT
OB920_09545	GT75(5-374)	-	GT
OB920_09570	GT2_Glycos_transf_2(14-164)	-	GT
OB920_09800	GH9(157-612)	Tat/SPII	endoglucanase
OB920_09985	GH109(1-154)	-	D-glucoside 3-dehydrogenase
OB920_10135	PL1_2(99-283)+CBM13(477-615)	Tat/SPI	pectate lyase
OB920_10880	GT66(23-652)	-	GT
OB920_10920	CE4(5-119)	-	chitooligosaccharide deacetylase
OB920_11685	GT2_Glycos_transf_2(4-109)	-	GT
OB920_11805	GT2_Glycos_transf_2(7-175)	-	GT
OB920_11850	GT81(108-293)	-	GT
OB920_13550	GH3(94-319)	-	beta-xylosidase
OB920_13785	CBM13(107-261)	Sec/SPI	CBM
OB920_13885	GH10(91-403)	Tat/SPI	endo-1,4-beta-xylanase
OB920_14610	GT20(25-496)	-	GT
OB920_14830	GT2_Glycos_transf_2(9-185)	-	GT
OB920_14850	CBM35(408-521)	Tat/SPI	CBM
OB920_15560	GH2(9-557)	-	beta-galactosidase
OB920_15950	GH5_8(81-278)	Tat/SPI	endo-1,4-beta-mannosidase
OB920_16560	CE15(38-429)	-	carbohydrate esterase
OB920_16960	GT2_Glycos_transf_2(7-111)	-	GT
OB920_16965	GT4(198-343)	-	GT
OB920_16970	GT4(207-353)	-	GT
OB920_16980	PL12(374-512)	-	heparin-sulfate lyase
OB920_16985	GT4(220-374)	-	GT
OB920_17000	GT2_Glycos_transf_2(146-304)	-	GT
OB920_17400	GT2_Glycos_transf_2(61-169)	-	GT
OB920_17495	CE4(115-223)	Tat/SPII	chitooligosaccharide deacetylase
OB920_17560	GH81(82-708)+CBM56(801-940)	Tat/SPI	endo-1,3(4)-beta-glucanase
OB920_17715	GH2(3-785)	-	beta-mannosidase
OB920_18365	GT4(165-298)	-	GT
OB920_18845	CE1(25-275)	-	esterase
OB920_18985	GH95(8-740)	-	alpha-L-fucosidase
OB920_18995	GH43_12(5-279)	-	alpha-L-arabinofuranosidase
OB920_19135	GH42(6-398)	-	beta-galactosidase
OB920_19540	GH15(291-652)	-	unknown
OB920_19545	GH13_20(289-575)	-	alpha-amylase
OB920_19595	GT87(69-311)	-	GT
OB920_19985	CBM13(3-90)	-	CBM
OB920_19990	GH11(77-250)+CBM13(288-423)	Tat/SPI	endo-1,4-beta-xylanase
OB920_19995	GH10(109-407)+CBM6(512-648)	Tat/SPI	endo-1,4-beta-xylanase
OB920_20000	GH11(39-213)	Tat/SPI	endo-1,4-beta-xylanase
OB920_20005	GH11(75-249)+CBM6(303-439)	Tat/SPI	endo-1,4-beta-xylanase
OB920_20010	CBM85(75-210)+GH10(281-584)	Sec/SPI	endo-1,4-beta-xylanase
OB920_20015	GH67(8-688)	-	alpha-1,2-glucuronosidase
OB920_20075	GH43_12(4-279)	-	alpha-L-arabinofuranosidase
OB920_20130	GH2(7-659)	-	beta-galactosidase
OB920_20140	GH51(3-495)	-	alpha-L-arabinofuranosidase
OB920_20170	GH127(17-560)	-	beta-L-arabinofuranosidase
OB920_20255	CBM67(342-509)+GH78(536-1041)	-	alpha-L-rhamnosidase
OB920_20260	GH4(17-195)	-	alpha-galacturonidase
OB920_20275	CBM13(454-592)	Tat/SPI	CBM
OB920_20280	GH43_3(45-332)+CBM13(411-547)	Tat/SPI	endo-alpha-1,5-L-arabinanase
OB920_20300	GH3(93-316)	-	beta-xylosidase